iScience

CellPress
OPEN ACCESS

Article

Serotonin-1A receptor, a psychiatric disease risk factor, influences offspring immunity via sex-dependent genetic nurture

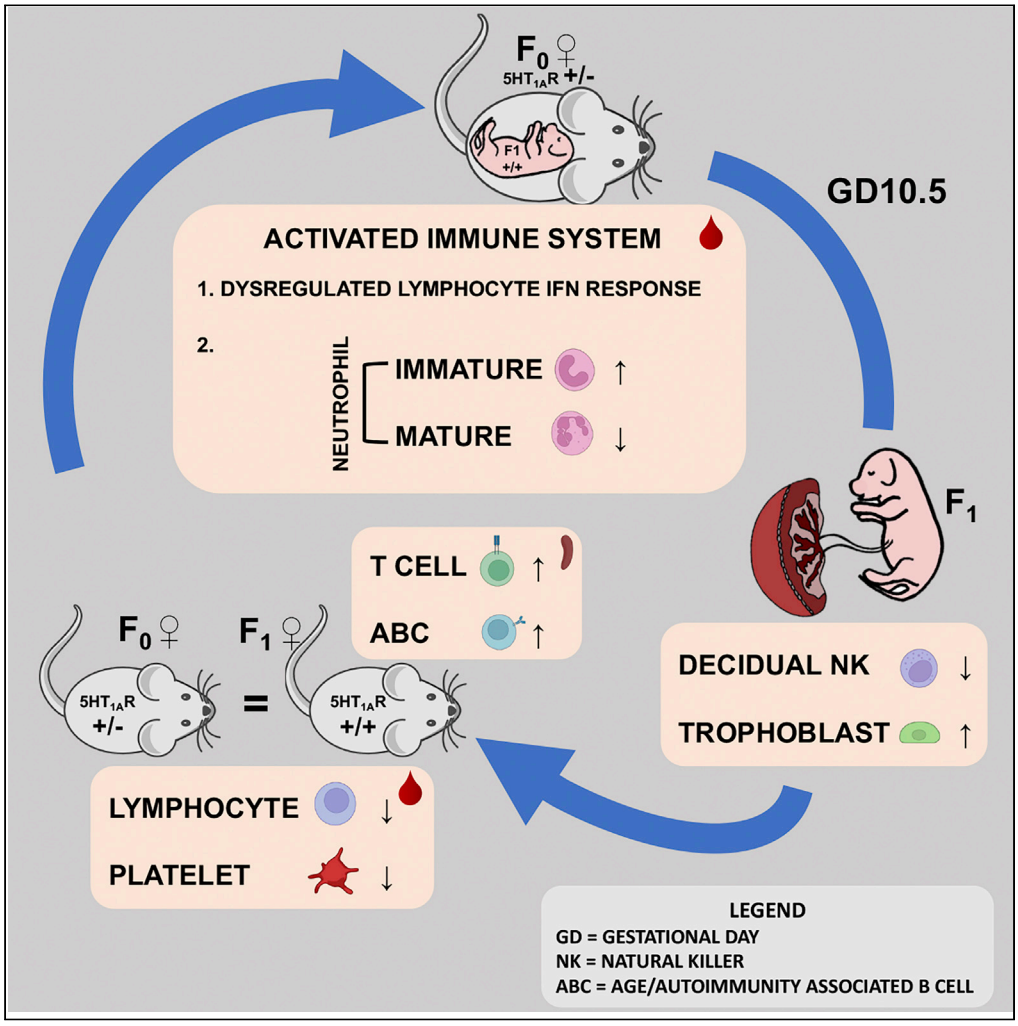

Rosa J. Chen, Anika Nabila, Swati Phalke, ..., Heidi Stuhlmann, Alessandra B. Pernis, Miklos Toth

mtoth@med.cornell.edu

Highlights

5HT1AR is a risk factor in anxiety and depression

5HT1AR is linked to immune system abnormalities in females

The 5HT1AR-immunity link is indirect and due to the dam's receptor deficit

The immune phenotype is associated with abnormal placental development

Chen et al., iScience 25, 105595
December 22, 2022
https://doi.org/10.1016/j.isci.2022.105595

iScience

CellPress
OPEN ACCESS

Article

Serotonin-1A receptor, a psychiatric disease risk factor, influences offspring immunity via sex-dependent genetic nurture

Rosa J. Chen,[1] Anika Nabila,[1] Swati Phalke,[2] Danny Flores Castro,[2] Judit Gal Toth,[1] Paul Bergin,[1] Jeroen Bastiaans,[3] Heidi Stuhlmann,[3] Alessandra B. Pernis,[2] and Miklos Toth[1,4,*]

SUMMARY

Serotonin-1A receptor (5HT1AR) is highly expressed in corticolimbic regions and its deficit is associated with anxiety and depression. A similar reduction in 5HT1AR heterozygous knockout (Het) mice results in anxiety-like and increased stress-reactivity phenotypes. Here we describe immunological abnormalities in Het females, characterized by an activated state of innate and adaptive immune cells. Het males showed only limited immune dysregulation. Similar immune abnormalities were present in the genetically WT female (F1) but not male offspring of Het mothers, indicating sex-specific immune system abnormalities that are dependent on the mother's 5HT1AR deficit, known as maternal genetic effect or "genetic nurture". Expression profiling of the maternal-fetal interface revealed reduced immune cell invasion to decidua and accelerated trophoblast migration. These data suggest that 5HT1AR deficit, by altering the maternal immune system and midgestational *in utero* environment, leads to sex-biased outcomes, predominantly immune dysregulation in the female and anxiety-like behavior in the male offspring.

INTRODUCTION

Among the 14 known serotonin receptor subtypes in mammals, 5HT1AR is of particular interest due to its possible role in the development of affective and mood disorders.[1] 5HT1AR exists in two populations in the brain. Autoreceptors are expressed presynaptically in 5HT neurons in the raphe nuclei of the brainstem, whereas heteroreceptors are expressed postsynaptically in the projection areas of 5HT neurons.[2] Human imaging and postmortem studies have found an association between reduced 5HT1AR heteroreceptor binding potential and anxiety, stress disorders, depression, and suicide completion.[3–5] In addition, the G allele of the C(-1019)G polymorphism in the *HTR1A* gene (encoding the 5HT1AR)[6] was associated with not only less receptor mRNA in the prefrontal cortex of nonpsychiatric control subjects,[7,8] but also anxiety disorders, major depression, substance abuse, and suicide attempts.[7,9,10] However, some studies reported increased 5HT1AR binding in individuals with drug-naïve major depression and bipolar depression, particularly in autoreceptors[6,11–15] indicating that the relationship between 5HT1AR and neuropsychiatric disease is complex and is dependent on, at least partly, whether the pre- or the postsynaptic receptor pool is altered.

Similar behaviors were also observed in mice with a partial and/or complete loss of 5HT1AR expression. We reported that 5HT1AR heterozygote (Het) and homozygote receptor knockout (KO) mice on the outbred Swiss Webster (SW) background exhibit anxiety-like behavior in the elevated plus maze (EPM) and increased stress reactivity, indicated by increased escape-directed behavior, in the forced swim test (FST).[16] Ramboz et al. generated 5HT1AR KO mice on the inbred 129/Sv background that displayed elevated anxiety-like behavior and increased stress-reactivity, whereas Het mutants exhibited only intermediate phenotypes in some of these behavioral tests.[17] Likewise, KO but not Het 5HT1AR mice, generated on the inbred C57BL/6J background by Heisler et al., displayed anxiety and increased stress reactivity.[18] These data show that only outbred Het SW mice (with a ~50% reduction in receptor density) exhibit anxiety (Figure 1A) that recapitulates the increased psychiatric disease risk of individuals with an up to 50% reduction in receptor binding potential.[3–5]

[1]Department of Pharmacology, Weill Cornell Medicine, New York, NY 10065, USA

[2]Center for Genomic Research at Hospital for Special Surgery, New York, NY 10065, USA

[3]Cell and Developmental Biology, Weill Cornell Medicine, New York, NY 10065, USA

[4]Lead contact

*Correspondence: mtoth@med.cornell.edu

https://doi.org/10.1016/j.isci.2022.105595

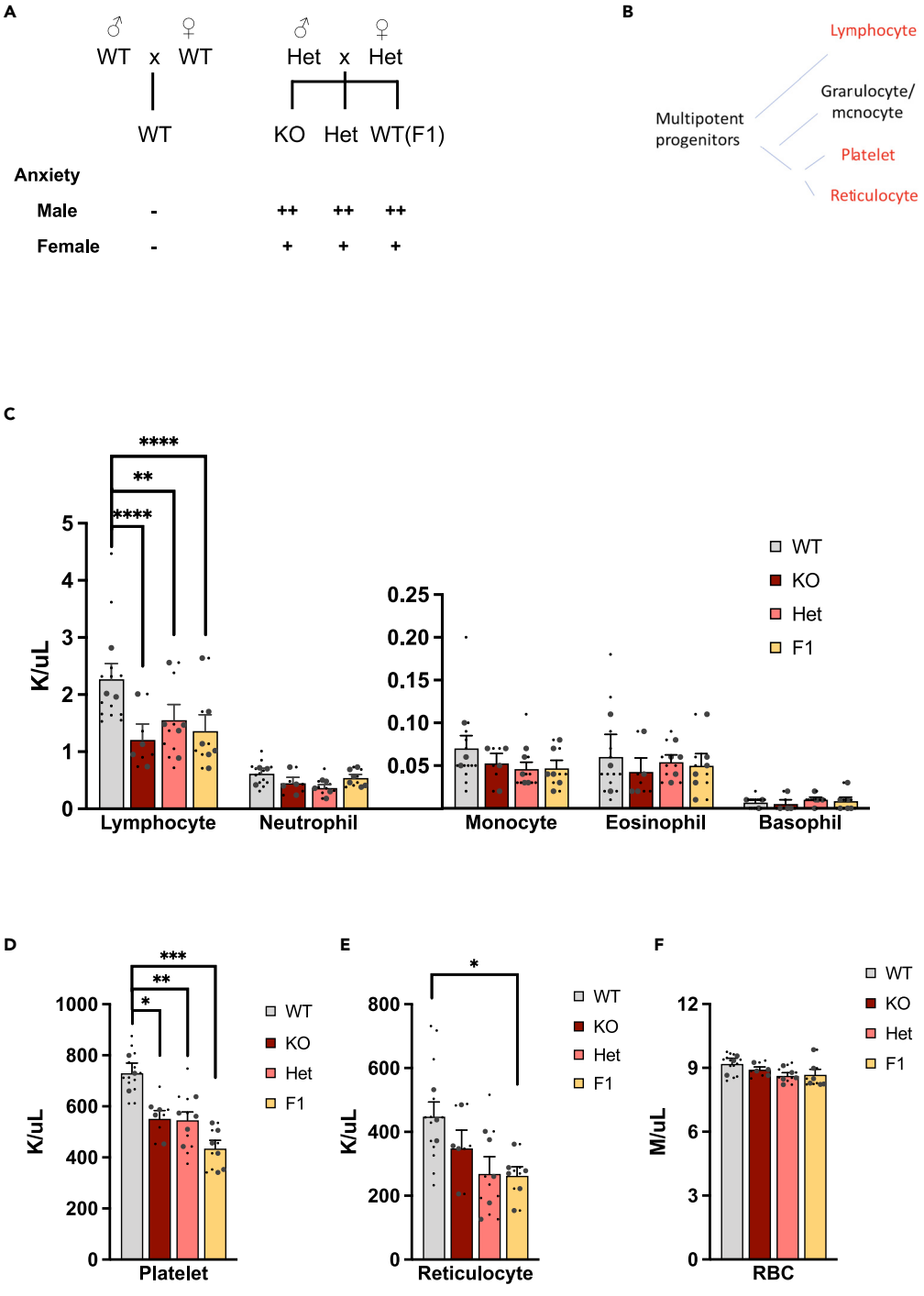

Figure 1. 5HT1AR deficient females exhibit cytopenia

(A) Generation of Het, KO and WT (F1) animals by crossing Het parents. WT animals were also generated by breeding an independent line. Male KO, Het and F1 mice exhibit more robust anxiety than females as reported.[19]

(B) Schematic representation of the origin of blood cells. Red highlight indicates cells affected in F1 females.

(C) Whole blood cell (WBC) differential. Reduced lymphocyte count in KO, H, and F1, relative to WT mice (two-way ANOVA, group-cell type interaction: $F(3,70) = 2.467$ $p = 0.0693$; Dunnett post hoc, WT vs KO $p = 0.0001$, WT vs Het $p = 0.0031$, WT vs F1 $p = 0.0011$). Small dots represent individual animals and large dots represent litter/maternal averages. Bar graphs are shown as litter mean ± SEM and statistics is based on litter means.

Figure 1. *Continued*
(D) Reduced platelet counts in KO, H, and F1 mice (ANOVA, F(3,14) = 10.83 p = 0.0006; Dunnett post hoc, WT vs KO p = 0.0161, WT vs Het p = 0.0100, WT vs F1 p = 0.0002).
(E and F) Reduced reticulocyte but normal RBC counts in F1 mice (ANOVA F(3,14) = 2.944 p = 0.0695; Dunnett post hoc, WT vs F1 p = 0.0429).

Our previous work also suggested that 5HT1AR deficit is associated with an abnormal immune phenotype in SW females, specifically with a reduced count of blood cells, i.e., cytopenia.[19] The dual behavioral-immune phenotype associated with 5HT1AR deficit in mice is in agreement with the frequent comorbidity between psychiatric and immune system diseases. Individuals with immunological disorders, such as rheumatoid arthritis, inflammatory bowel disease, and multiple sclerosis have an above chance likelihood for prior diagnosis of depression, anxiety, bipolar disorder, and schizophrenia.[20] The association seems to be bidirectional, as individuals with immune disorders have an increased risk for developing psychiatric disease.[21] Although surveillance bias or challenges living with a chronic condition may play a role, comorbidity could be due to common etiology. Indeed, preclinical studies show that early life immune activation produces both immunological and behavioral abnormalities in rodents and non-human primates.[22,23]

The possibility that the neuropsychiatric disease risk factor 5HT1AR may cause an immune system abormality prompted us to investigate the immune system of Het mice. Our data suggest that the immune phenotype of Het females is caused by their mother's receptor deficit via altering the maternal immune and placental environment. In a similar manner, Het mothers program their genetically WT female offspring to exhibit immune abnormalities. These findings are most compatible with "genetic nurture"[24] by which the parental genotype shapes the parental environment to influence offspring outcomes.

RESULTS

Female 5HT1AR deficient mice exhibit cytopenia

Adult 5HT1AR Het and KO females exhibit lymphocytopenia and thrombocytopenia (Figures 1C and 1D; Mitchell et al. 2016[19]). In contrast, the number of reticulocytes and red blood cells (RBCs) were not significantly reduced in Het and KO females (Figures 1E and 1F). Lymphocytopenia and thrombocytopenia in Het and KO females were comparable indicating that a partial loss of the receptor in Het females was sufficient to elicit the phenotypes. Het males had normal lymphocyte count but exhibited thrombocytopenia (Figures S1A and S1B). These data show a cytopenia phenotype that involves two hematopoietic lineages (lymphoid and megakaryocytic) in Het females (Figure 1B).

Female cytopenia is caused by parental 5HT1AR deficit

We previously reported and here reproduced that the offspring of Het mothers and Het fathers, including the genetically WT (henceforth F1) offspring (Figure 1A), also have cytopenia, relative to the WT offspring of WT parents. Specifically, F1 WT females, like their Het littermates, exhibited lymphocytopenia and thrombocytopenia (Figures 1C and 1D). F1 and Het males exhibited a lesser phenotype as they had a normal lymphocyte count but reduced number of platelets (Figures S1A and S1B). This suggests that cytopenia is not directly related to the individual's receptor expression but rather, to the parents' 5HT1AR deficit, a phenomenon referred to as "genetic nurture".[24] Of note, anxiety that predominantly affects the male offspring has a similar pattern of programming, with Het and F1 offspring exhibiting comparable behavioral abnormality, as we reported earlier[19,25] (Figure 1A). Despite these immunological and behavioral phenotypes in the offspring, maternal 5HT1AR deficit had no effect on litter size, offspring weight at birth, survival, and offspring development.[26]

In addition to lymphocytopenia and thrombocytopenia, F1 females exhibited cytopenia in the erythroid lineage, specifically reticulocytopenia but without anemia (Figures 1E and 1F). This was unexpected because Het and KO females had no statistically significant reduction in reticulocyte count (Figure 1E), suggesting that in the partial or complete absence of 5HT1AR in the offspring, the Het parental effect on thrombocytopenia is mitigated. This is reminiscent of "genetic compensation" when loss of function of one gene compensates for the loss of function of another gene,[27] except that here, a non-genetic Het parental effect on the erythroid lineage seems to be moderated by the disruption of the *Htr1a* gene in the offspring. Again, F1 males exhibited no phenotype as they had a normal reticulocyte count (Figure S1C).

Cytopenia of the female F1 and Het offspring is originated from the Het mother

Because of its preferential manifestation in females, we hypothesized that offspring cytopenia is related to the mother's, rather than the father's, 5HT1AR deficit. We replaced Het mothers with WTs in pair breeding with Het fathers to test if cytopenia is no longer exhibited in the F1 offspring. Indeed, WT female offspring of Het fathers (and WT mothers) showed no significant lymphocytopenia, thrombocytopenia, and reticulocytopenia (Figures S2A, S2C, and S2E). This is in contrast with the lymphocytopenia, thrombocytopenia, and reticulocytopenia of F1 female offspring of Het mothers, as shown in Figures 1C and 1E. We concluded that F1 female cytopenia is due to the maternal and not paternal 5HT1AR deficit. Lack of cytopenia in genetically Het females inheriting the mutant receptor gene from their father (Figures S2A, S2C, and S2E) also strengthens the previous conclusion that the individual's own receptor deficit does not cause the phenotype.

The Het mother - F1 WT daughter transmission of cytopenia suggests a similar transmission from the Het grandmother to the Het mother, because cytopenia is related to the maternal but not the individual's Het 5HT1AR genotype. Indeed, Het females that in our breeding scheme are considered the mothers of the F1 offspring (Figure 1A) exhibited cytopenia if their mothers, i.e., grandmothers in the linage, were Het (Figures 1C and 1D) but not when the grandmothers were WT (Figures S2A and S2C).

Next, we cross-fostered F1 females at birth to WT mothers and WT females to Het mothers and found that the postnatal Het maternal environment was sufficient to program reticulocytopenia in females (Figure S3C). However, exposure to the prenatal or the postnatal Het environment resulted in no lymphocytopenia and thrombocytopenia suggesting that both prenatal and postnatal Het environment may be necessary for maternal programming of these phenotypes (Figures S3A and S3B). As we reported earlier,[25] anxiety of males was also transmitted to the F1 offspring from their Het mothers nongenetically, but it was programmed during prenatal life. This indicates that, beside their sex biased nature, the behavioral and immunological phenotypes may follow different non-genetic transmission patterns.

Although none of the three types of cytopenia was transmitted by the Het father to the F1 female offspring, male F1 and Het offspring acquired reticulocytopenia through the male line (Figure S2F). Therefore, reticulocytopenia is acquired by females from their Het mother postnatally and by males from their Het father (Figures S2F and S3C).

Autoantibodies are not elevated in F1 and Het females

Cytopenia can be caused by antibody-mediated autoimmunity in systemic autoimmune disease, such as systemic lupus erythematosus.[28,29] However, we found no or slightly reduced levels of IgG and IgM anti-dsDNA, anti-cardiolipin, and anti-phosphatidylserine antibodies in F1 and Het relative to WT females, that were all very low compared to the significantly increased antibody levels in two mouse lines with an SLE-like autoimmune condition[30] (Figure S4).

Expansion of T and subsets of B lymphocyte populations in the spleen of F1 but not Het females

Next, we tested if the peripheral lymphocytopenia of F1 females is mirrored in the resident lymphocyte population in the spleen, a secondary lymphoid organ perfused with a continuous flow of immune cells from the periphery. Circulating T and B lymphocytes traffic and position within defined splenic microenvironments.[31] Because we were interested in the potential life-long impact of parental 5HT1AR deficit on the immune system and because immune dysfunctions tend to manifest later in life, we used older mice (>24 weeks of age).

Multi-parameter flow cytometry showed that both the proportion of $CD3^+$ splenocytes (representing all T cells) relative to all splenocytes and their overall number were unchanged in Het females but were increased in F1 females (Figures 2A, 2B, and S5), indicating a Het parental effect which is suppressed when combined with a deficit in 5HT1AR, initially observed with reticulocytes (Figure 1E). A similar pattern was seen in the population of $CD3^+CD4^+$ T helper cells (Figures 2B and S5). Relative proportion and number of memory $CD4^+$T cells, expressing the activation marker $CD44^+$, were also increased in F1 but not Het females. Further, similar increases in relative proportion and cell number were seen in $CD4^+$ follicular T helper (Tfh) cells residing in B cell zones in the spleen. These cells play key roles in T-dependent antibody responses and their dysregulation have been implicated in autoimmunity.[32] However, the regulatory subset of follicular T cells (Tfr) had a similar proportional increase, maintaining the Tfh/Tfr ratio unchanged and thus likely mitigating the potential autoimmune effect of the expanded effector Tfh population (Figure 2B).

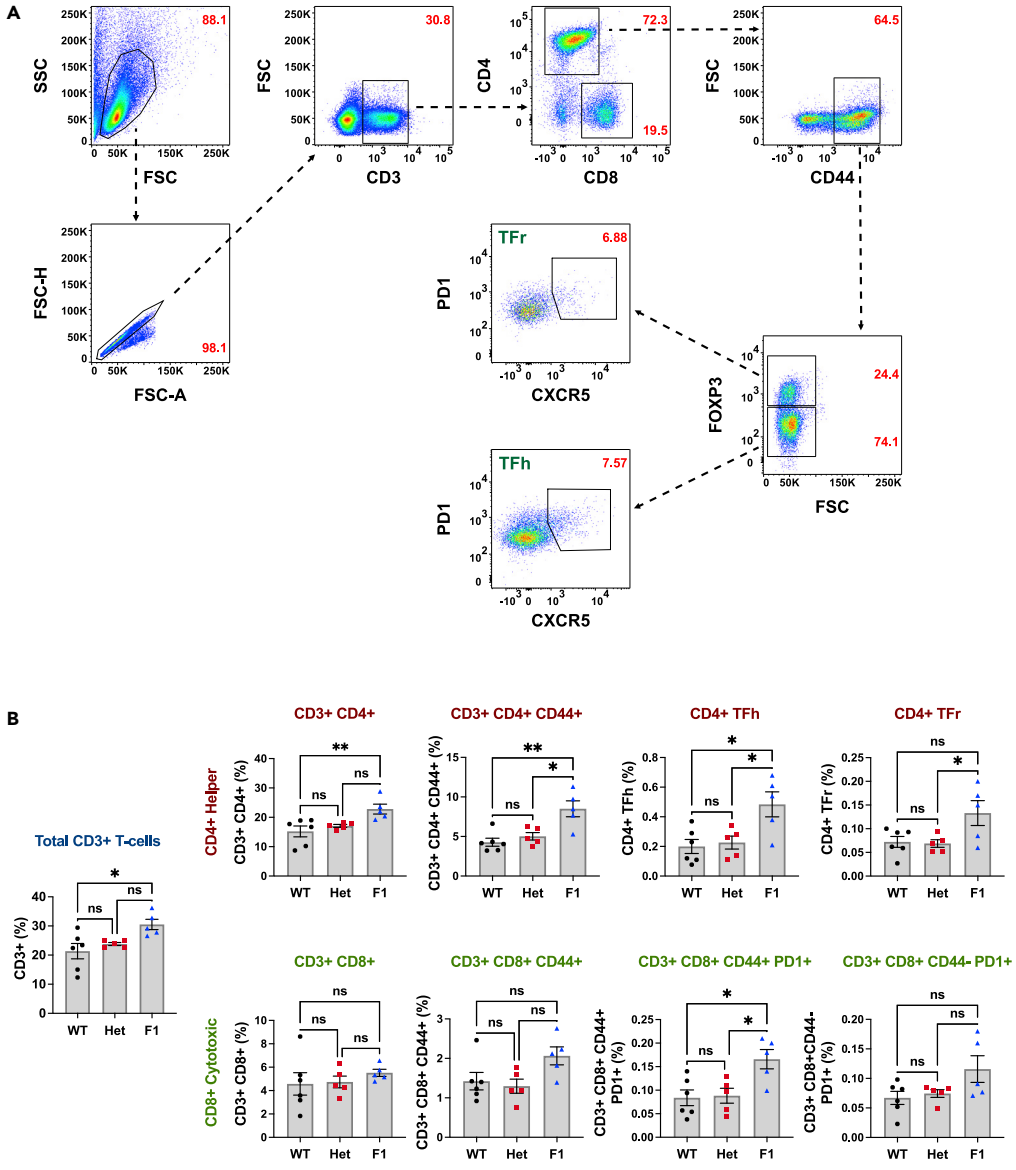

Figure 2. Het parental environment increases the proportion of all T cells ($CD3^+$) and some T cell subpopulations within splenocytes in F1, but not Het female offspring

(A) Gating strategy for profiling T cell populations from spleen, including T follicular regulatory (TFr) and T Follicular helper (TFh) cells. Lymphocytes were gated based on their forward (FSC) and side scatter (SSC), and aggregates (doublets and other conjugates) were excluded by using forward scatter area (FSC-A) and forward scatter height (FSC-H). $CD4^+$, $CD8^+$, TFr and TFh populations were gated based on the presence of specific markers as indicated.

(B) Frequencies of T cell subsets in % of all splenocytes are indicated on the y axis. Each dot represents an individual mouse from a different mother (ANOVA, Tukey post-hoc, *$p < 0.05$, **$p < 0.01$). ns, no significance. Bar graphs are shown as mean ± SEM.

Indeed, F1 females had WT like baseline autoantibody levels, as shown in Figure S4. $CD8^+$ cytotoxic T cell populations, representing the other major T cell lineage, were unchanged in F1 and Het females, except a proportional increase in $CD8^+CD44^+$ PD-1^+ (programmed cell death-1) T cells (Figure 2B). Overall, these data indicate the expansion of the total T cell population within splenocytes that involves mostly the $CD4^+$T cell lineage suggesting a parental receptor genotype effect at or before the maturation of helper T cells. These changes may indicate enhanced T cell activity.

A similar analysis with B lymphocyte populations that included mature and immature B cells, marginal zone B cells, follicular zone B cells, germinal center B cells, and plasma cells revealed no changes in F1 and Het

females, relative to WT females (Figure S6). This suggests that in contrast to the broad T lymphocyte effect, the parental receptor genotype had no effect on B cells. However, a unique small subset of B cells, age/autoimmunity associated B cells or ABCs,[33] exhibited a significant increase in F1 but not Het females (Figure S6).

Given the peripheral lymphocytopenia of Het and F1 females, the increases in lymphocyte populations in the spleen might suggest compensation or altered distribution of cells between the blood and spleen. However, only F1 females showed the increase in splenic lymphocytes, whereas both H and F1 females exhibited lymphocytopenia, suggesting no direct connection between the reduced number of peripheral lymphocytes and the increased number of splenic lymphocytes in F1 females. Indeed, factors regulating the dynamics of the two pools are quite distinct.[31]

Immune status of Het females during pregancy

Because all data pointed toward the maternal receptor deficit as a cause of the immunlogical abnormalities, we next focused on the gestational maternal environment. Maternal immune and placental cells are especially relevant because they are in close contact with the developing embryo. In these studies, we used scRNA-Seq (10X Genomics) because this technology, via gene expression profiling, can identify not only the idenitty but also the cellular state of individual cells in a population of mixed cells.

We profiled peripheral blood mononuclear cells and granulocytes from Het and WT females at (mid)gestation day (GD)10.5 to a depth of 25,000–30,000 reads per cell (Figure 3A). A total of 2,026 Het cells and 1,448 WT cells that passed quality control were clustered and then visualized by Uni-form Mani-fold Approximation and Projection (UMAP). We identified 18 leukocyte clusters, which corresponded to known cell types such as lymphocytes (three B cell and seven T cell types), natural killer (NK) cells, dendritic cells (DC), monocytes (classical, intermediate, and nonclassical),[34] and neutrophils (G3 and G4 immature and G5 mature)[35] (Figure 3B and Table S1 for cluster markers). We found 40 differentially expressed genes (DEGs, >1.5-fold change, adjusted $p < 0.05$) in Het, relative to WT cells across several clusters or in single clusters (Table S2). Most prominently, 35% of DEGs belonged to interferon I regulated genes (IRGs, www.interferome.org)[36] such as *Ifi27L2a* (in $CD4^+$T cells, mature neutrophils, and nonclassical monocytes), *Ifi202b* (classical monocytes), and *Ifitm3* (G4 immature neutrophil) (Figure S7). Interferon I is a potent regulator of innate and adaptive immunity and the enrichment of DEGs in IRGs suggested activated or dysregulated interferon signaling and immune homeostasis in both innate and adaptive immune cells in Het females. Further, upregulation of *Klra1, 4,* and *8*[37] in NK cells, encoding inhibitory Ly49G, and activating Ly49H and Ly49D membrane glycoprotein receptors respectively, suggested heightened immune reactivity/surveillance via their interaction with class I major histocompatibility complex-I (MHC-I) on normal and altered cells[37] (Table S2). Specifically, "educated" NK cells are cytotoxic toward altered cells through activating Ly49 receptors while tolerant toward cells that express self-MHC-I through their inhibitory Ly49 receptors.[37]

Further, scRNA-Seq revealed a dramatic change in the population structure of neutrophils in pregnant Het females (Figures 3B clusters N1-3 and 3G). Although immature G3 neutrophils[35] (expressing the secondary granule genes *Camp*, *Ltf* and *Ngp*) and more mature G4 neutrophils (expressing *Retnlg*) were present in very low numbers in WT blood as expected, Het female blood contained larger numbers of these normally bone marrow (BM) resident cell types[38] (Figures 3B clusters N1 and N2, 3C-E and 3G). In contrast, the G5 mature neutrophil population (expressing *Il1b*), which is the prominent neutrophil class in the periphery, was decreased in Het relative to control WT blood (Figures 3B cluster N3, 3C, 3F, and 3G). Of note, complete blood count did not detect the change in neutrophil population structure because it cannot differentiate between immature and mature neutrophils. The neutrophil population structure of Het dams was reminiscent of that reported in mice infected intraperitoneally by *E. coli*.[35] Infected mice exhibited increased migration of mature neutrophils from the periphery to target tissue as well as accelerated maturation and increased release of maturating neutrophils from the BM to the periphery. We concluded that both the expression profile of peripheral leukocytes and the population structure of neutrophils point to an activated immune system in Het females/mothers.

Increased trophoblast invasion to the decidua in Het pregnancy

Next we analyzed the decidua, the maternal interface to the embryo that is composed of maternal immune cells, epithelial cells, blood vessels, and decidual stromal cells or DSCs.[39] We used single nuclei for transcriptional profiling because RNA integrity was better preserved during nuclei preparation than during cell dissociation. We profiled 9,955 and 13,120 nuclei from dissected WT and Het maternal deciduas (of

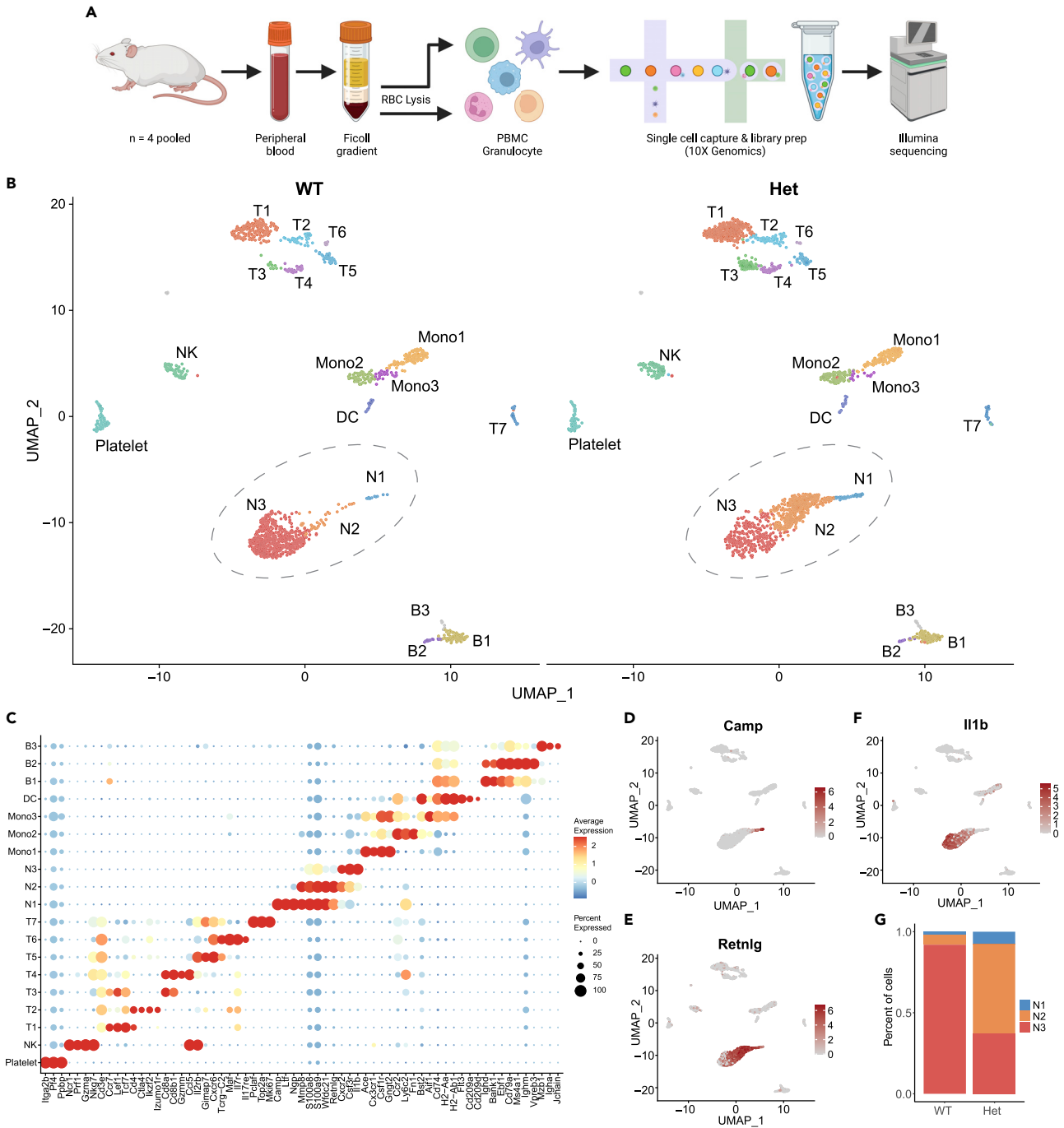

Figure 3. ScRNA-Seq profiling of GD10.5 Het and WT peripheral leukocytes

(A) Workflow of scRNA expression profiling from purified PBMCs and granulocytes.

(B) UMAP of Het and WT GD10.5 blood leukocytes. Each dot represents one cell colored according to assignment by clustering analysis. B1-3, B cell clusters; T1, Naive CD4$^+$T cells; T2, Regulatory T; T3, Naive CD8$^+$ T; T4, Cytotoxic CD8$^+$ T; T5, IFNγδ T; T6, IL17γδ T; T7, Proliferating T cells; NK, NK cells; DC, Dendritic cells; N1, Neutrophil 1/Immature G3; N2, Neutrophil 2/Immature G4; N3, Neutrophil 3/Mature G5; Mono1, Nonclassical monocytes; Mono2, Classical; Mono 3, Intermediate. N1-N3 clusters are circled because of dramatic change in the population structure.

(C) Dot plot showing average expression and percent of cells in each cluster expressing marker genes for each cluster. Genes listed on the xaxis and clusters on the yaxis.

(D–F) Expression of cluster markers in N1-N3 populations: *Camp*, secondary granule gene; *Retnlg*, encodes resistin-like gamma, which is involved in myeloid dendritic cell chemotaxis; *Il1b*, interleukin 1 cytokine that regulates inflammatory response, respectively.

(G) Altered proportions of mature (N3) and immature (N1 and N2) neutrophils in Het blood.

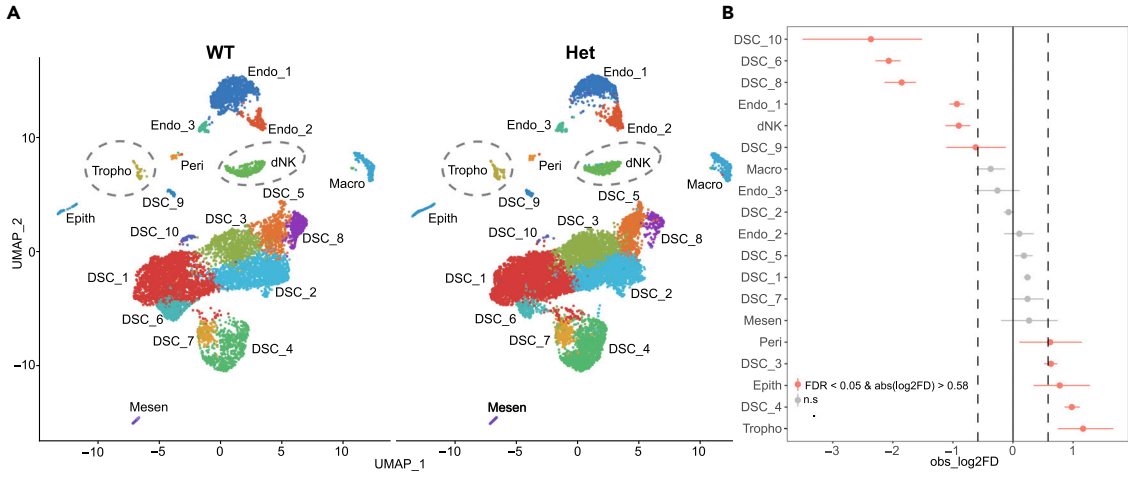

Figure 4. SnRNA-Seq profiling of GD10.5 Het and WT decidua

(A) UMAPs. Decidual stromal cells, DSCs; endothelial cells, Endo; decidual NK cells, dNK; macrophages, Macro; trophoblasts, Tropho; mesenchymal cells, Mesen; epithelial cells, Epith; pericytes, Peri. Circles indicate a trophoblast and a dNK cell cluster exhibiting an increase and a decrease in cell number in Het decidua, respectively.

(B) Cell types with significantly increased (+) and reduced (–) proportions in Het vs WT decidua (e.g., + and – fold difference, FD, respectively). Horizontal bars represent confidence interalls 5% and 95%.

female WT and F1 placentas), respectively. Based on known markers, we identified all major decidual cell types that included 10 clusters of DSCs, 3 clusters of endothelial cells, and single clusters of decidual NK (dNK) cells, macrophages, trophoblasts, mesenchymal cells, epithelial cells, and pericytes[40–42] (Figures 4A, S8, and Table S3 for cluster markers). The number of cells in four small DSC clusters was reduced in the decidua of Het/F1 female placenta, whereas increased in two larger clusters, resulting in a slight increase in the overall population of DSCs in Het (~81% of all cells) vs WT (~75%) deciduas (Figure 4B DSC_6, 8, 9, 10 and DSC_3, 4). In contrast, the single population of dNK cells, which normally represent 70% of lymphocytes in the uterus,[43] was reduced (Figure 4B "dNK"). The other significant immune cell type, macrophage, showed no numerical change in Het decidua, but its DEGS were enriched in the biological function of "regulation of phagocytosis" (27.32-fold; FDR 9.67E-03). Because all the DEGs in this biological function (*Sirpa, Ptprj, Pparg, Ptprc, Cd300a*) are positive regulators of phagocytosis and were downregulated, phagocytosis in Het decidua is likely impaired (Table S4). This change, combined with the reduced number of dNK cells, may indicate a deficit in decidual immunity.

Finally, we found an increased number of trophoblast cells, identified by the expression of *Plac1* (Placenta Enriched 1), in GD10.5 Het deciduas (Figures 4B, "Tropho" and S8), an unexpected finding because trophoblast invasion to the decidua in mice begins later, around GD14.[44] Premature invasion of trophoblasts to the decidua from the fetal compartment indicated a placental abnormality beyond the changes in decidual immune cells.

Next, we performed immunostaining to determine the identity and localization of trophoblasts in Het decidua. We found clusters of cells positive for the pan-trophoblast marker TPBPA in GD10.5 Het but not WT decidua (Figures 5A and 5C, higher magnification 5B and 5D). In normal pregnancy at GD10.5, TPBPA positive trophoblasts are restricted to the junctional zone (JZ), as was clearly visible in WT placentas. The JZ is the middle compartment of the placenta,[45] involved in hormone secretion (e.g., prolactin family members) and metabolism (e.g., glycogen storage).[46,47] The presence of TPBPA immunopositivity in Het decidua confirmed the snRNA-Seq data and indicated disorganized JZ development that extends to the decidua, or premature JZ trophoblast invasion. Because NK deficiency is known to be associated with increased trophoblast invasion,[44] and given the reduced number of dNK cells in Het decidua, the decidua abnormality could be because of accelerated trophoblast invasion.

Although the presence of TPBPA positive trophoblasts in GD10.5 Het decidua indicated a placenta abnormality at midgestation, by GD17.5, following the naturally occurring invasion and expansion of JZ trophoblasts in normal pregnancies from GD14 onward, the Het decidua became structurally similar to that of WT

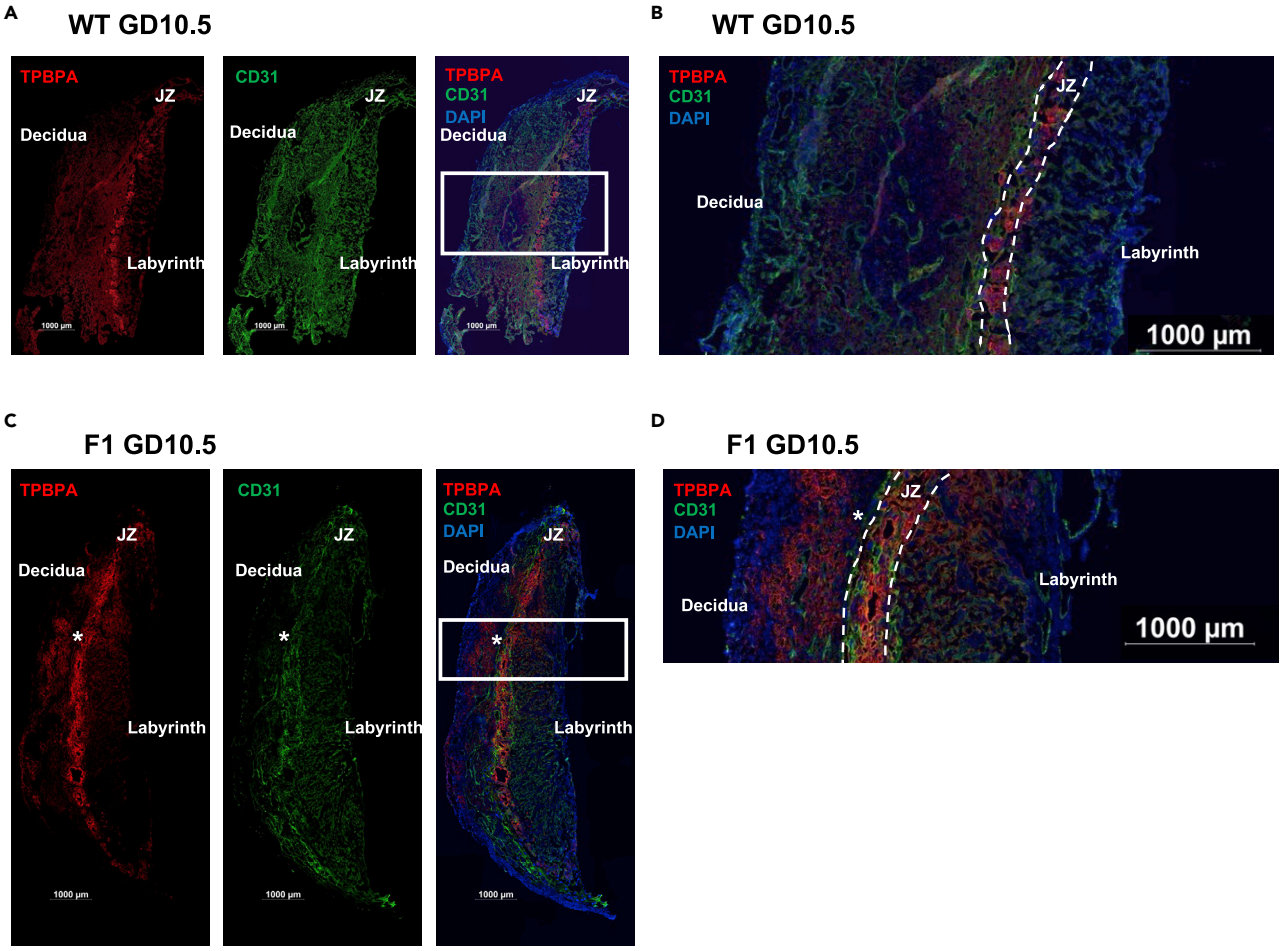

Figure 5. Premature onset of JZ trophoblast invasion into the decidua in Het pregnancy

(A) WT placenta of WT mothers stained for the JZ trophoblast marker TPBPA (left), blood vessel endothelial cell marker CD31 (middle), and both together with DAPI counterstaining (right).

(B) Higher magnification of merged images from "a". Dashed lines indicate the JZ boundaries.

(C) Same as "a" but with F1 placenta in Het pregnancy. Star indicates a TPBPA positive area in the decidua.

(D) Higher magnification of merged images from "c".

(Figures 6A and 6B). This may explain the apparent lack of intrauterine growth retardation[26] that is often associated with placental abnormalities.

Expression of the 5HT1AR in immune cells

The activated immune and expanded JZ phenotypes of Het mothers suggested that proper 5HT1AR signaling in hematopoietic/immune and placental cells may be required for the development of the immune system and placenta. Expression of *HTR1A* transcripts was reported in human peripheral lymphocytes from healthy individuals in some studies,[48] in particular following mitogen stimulation,[49] but not in another study.[50] Expression of the *Htr1a* gene in unstimulated mouse lymphocytes/splenocytes was also shown by an RNase protection assay but not PCR.[51] Analysis of *Htr1a* expression in publicly available databases suggested low or no detectable expression in mouse immune and hematopoietic cells. For example, lymphocytes and neutrophils and their progenitors did not express appreciable amounts of *Htr1a* mRNA in a microarray database[52] (Figure S9A). Similarly, RNA-Seq detected no *Htr1a* transcripts in mouse lymphoid progenitors in the bone marrow (BM).[53] However, *Htr1a* RNA was detected in 32N megakaryocytes, but the expression level was much lower than in brain[52] (Figure S9A). Also, a more recent single cell RNA-Seq profiling detected no appreciable number of megakaryocyte progenitors expressing *Htr1a* transcripts in mouse BM[54] (Figure S9B). We also measured total plasma 5HT levels because platelets

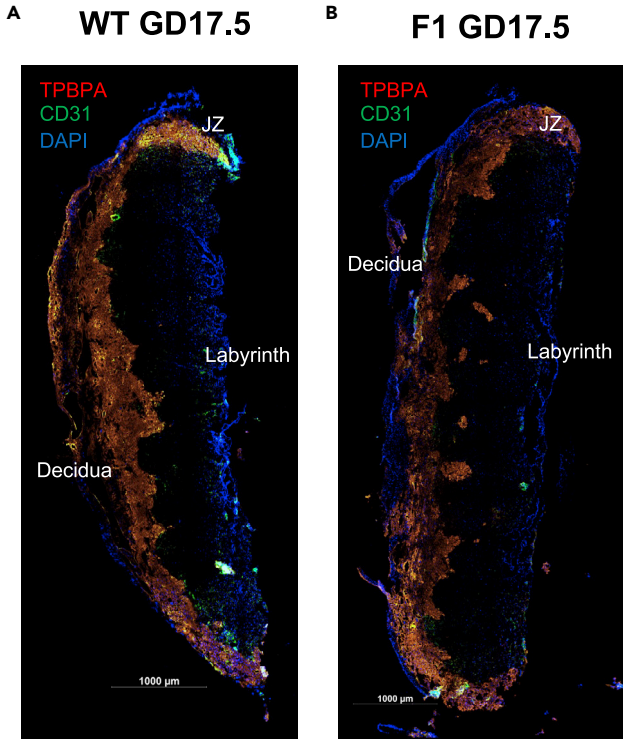

Figure 6. Morphology of F1 placenta is normalized by GD17.5
(A and B) GD17.5 WT and F1 placentas stained for TPBPA, CD31, and DAPI.

take up and store 5HT, but found no difference between WT and Het females (Figure S9C). Further, *Htr1a* RNA expression was detected at a low level in reticulocytes by microarrays[52] and in erythroid progenitors in fetal liver by RNA-Seq[54] (Figures S9A and S9D), but it was lower than in brain. Further, expression of the 5HT1AR protein from a low baseline in unstimulated mouse lymphocytes to a higher level after mitogen stimulation was also reported in.[51] Finally, we detected no *Htr1a* expression in trophoblasts in our snRNA-Seq profiling of the decidua. Overall, these data indicate a low expression of the *Htr1a* gene and 5HT1AR protein in mouse immune and hematopoietic cells that, however, could be still significant functionally. Because there is no direct correlation between a receptor deficit and the immune phenotype (as the genetically WT F1 offspring is affected), we hypothesize that a reduction in 5HT1AR signaling in Het female immune cells may alter the maternal environment that in turn leads to the placental and offspring immune phenotypes.

Alternatively, changes in the Het maternal immune system and placenta, and the consecutive programming of offspring, could be caused by reduced receptor levels in the Het female brain. In contrast to its low expression in the hematopoietic and immune system, 5HT1AR is highly expressed in the brain, particularly in the limbic system, cortex, and raphe nuclei. Although this potential link has not been studied, circulating hormones of the neuroendocrine system (e.g., ACTH and glucocorticoids)[55,56] may represent a bridge between central 5HT1ARs and the maternal immune system. Reduced 5HT1AR in the medial hypothalamus has been linked to exaggerated ACTH responses to stress,[57] and chronic activation of the HPA axis via elevated levels of glucocorticoids may compromise the immune system by influencing the stimulus-responsiveness and trafficking of immune cells, including lymphocytes, neutrophils, and NK cells.[58,59] Indeed, we measured increased corticosterone levels after restraint stress in 5HT1AR Het females (Figure S10). Other brain-immune pathways that might be regulated by central 5HT1ARs include the autonomic nervous system, as pharmacological manipulation of 5HT1ARs has been reported to alter sympathetic tone.[60,61]

DISCUSSION

We report an unexpected relationship between 5HT1AR, a risk factor in psychiatric diseases, and the immune system. We found that female mice deficient in 5HT1ARs have significant disruptions in their

hematopoietic and immune systems. Further, the genetically WT offspring of Het mothers had similar and, in the spleen, even more robust immunological abnormalities. These findings indicate that immune abnormalities are not directly related to the individual's receptor expression but rather, to the mother's 5HT1AR deficit. Then, consequently the immune abnormalities in Het mothers are programmed by their Het grandmothers. This phenomenon is known as parental/maternal genetic effect[62] or more recently "genetic nurture" in humans.[24] For example, educational attainment, as well as nutrition- and health-related traits, were best described by parental genetic variations in a genome-wide association study.[24] Because these parental/maternal genetic effects are polygenic, the responsible genes and their effects on the maternal environment are not known. Here we found that a single gene, encoding the 5HT1AR, is linked to a genetic nurture effect on the hematopoietic/immune system of the offspring. Importantly, a partial reduction in 5HT1AR, similar to the reduction in receptor binding potential described in individuals with various neuropsychiatric disorders,[3–5,7,9,10] was sufficient to elicit the immune phenotype.

Although anxiety was also transmitted to the F1 offspring from their Het mother nongenetically, the immunological and behavioral phenotypes seem to follow different transmission paths, as development of anxiety was programmed during prenatal life whereas the immunological abnormalities also required a postnatal maternal effect, shown by cross-fostering experiments. The postnatal effect was unlikely related to maternal care as Het females had comparable arched-back nursing, licking and grooming of pups, pup retrieval and nest building behaviors to that of WT mothers.[26]

Because of the maternal transmission of the immune phenotype, we expanded our study to the female immune system during pregnancy, as well as to the maternal placenta eg., decidua. Circulating lymphocytes showed the activation/dysregulation of interferon induced genes whereas neutrophils expressed inflammatory genes. Also, we observed a reduction in dNK cells and an increase in trophoblasts in the decidua, reminiscent of the accelerated interstitial trophoblast cell invasion in NK cell deficient Tgε26 mice.[44] Notably, trophoblast cell invasion was also accelerated in mice deficient of interferon-γ (IFNγ) or IFNγ receptor,[44] indicating that dNK cell-derived IFNγ regulates trophoblast migration and that the deficit in dNK cells may have a causative relationship with the early onset of trophoblast invasion in Het decidua.

The F1 female offspring, in addition to exhibiting all the immunological abnormalities of the Het females, showed reticulocytopenia, more significant thrombocytopenia, and expansion of splenic T cells and a subset of B cells, suggesting a more exaggerated activation of the immune system and that the Het genotype may suppress the Het maternal effect. Expansion of ABCs in F1 females is especially noteworthy because formation of ABCs is particularly sensitive to the presence of innate signals like those mediated by TLRs (Toll-like receptors that recognize pathogen-associated molecular patterns).[33] Therefore, increased expansion of ABCs may reflect a change in the local inflammatory milieu.

Immune system abnormalities and the previously reported anxiety[63] of Het and F1 animals were sex specific. Het and F1 females exhibit strong immune phenotypes, whereas their anxiety is less robust (Figure 1A). In contrast, Het and F1 males have relatively unperturbed immunity but display robust anxiety. These data are consistent with the comorbidity of psychiatric diseases and immune-mediated inflammatory diseases,[20] as well as with the increased frequency of immune disorders in females,[64,65] and the elevated risk of males to develop neuropsychiatric disorders following intrauterine insults.[66] Overall, our data suggest that, when exposed to the same 5HT1AR deficient maternal environment, female littermates preferentially exhibit immune system abnormalities whereas male littermates exhibit robust anxiety (Figure 7). Our findings with Het females have human relevance as up to 50% reduction in receptor binding has been found in depression and stress disorders.[3–5,67–69] Therefore, a maternal 5HT1AR deficit may increase the risk for psychiatric conditions in males and immunological disease in females.

Limitations of the study

Although we were able to link maternal receptor deficit to the immune and placental abnormalities of the female offspring, the tissue and cell type origin of the relevant 5HT1AR pool in the mother remains unknown. 5HT1AR expressing maternal organs, tissues, and cells in direct contact or communication with the developing fetus may explain the maternal receptor-dependent offspring phenotypes. We considered immune cells in the Het maternal blood as their reduced signaling, via the placenta, could directly affect the development of the fatal/neonatal immune system. Indeed, both receptor transcripts and the receptor protein have been detected in mouse lymphocytes. However, expression of *Htr1a* was very low under resting

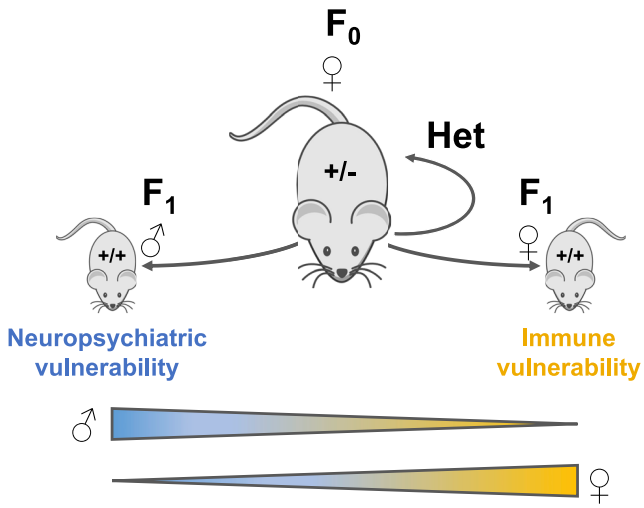

Figure 7. Summary model of sex-specific maternal programming of offspring phenotypes

Exposed to the same 5HT1AR-deficient maternal environment, female littermates exhibit immune system abnormalities and moderate anxiety whereas male littermates have no immune phenotype but robust anxiety.

conditions[51] and only mitogen stimulation or immune activation of these cells resulted in detectable levels in multiple studies.[48–51] Therefore, inflammation in Het mothers may increase receptor expression that, in turn, could mitigate effects of the receptor deficit. Placenta is also a reasonable candidate but we found no detectable expression in any decidual (e.g., maternal placental) cells in an snRNA-Seq experiment. In contrast, central neurons have much higher receptor expression than immune cells and may regulate, through hormones, cytokines and even neurotransmitters, the development of the offspring immune system.[70–73] Indeed, we show correlative data suggesting that the neuroendocrine system could be part of the mechanism linking maternal 5HT1ARs in the brain with the offspring immune/placenta phenotypes. Another possible mechanism that may connect the maternal brain with the placenta and offspring immune system is the autonomic nervous system. Whether any of these mechanisms explain the phenotypes, at least partly, will require further studies.

STAR★METHODS

Detailed methods are provided in the online version of this paper and include the following:

- KEY RESOURCES TABLE
- RESOURCE AVAILABILITY
  - Lead contact
  - Materials availability
  - Data and code availability
- EXPERIMENTAL MODEL AND SUBJECT DETAILS
  - *In vivo* animal studies
- METHOD DETAILS
  - Timed pregnancies
  - Complete blood count
  - Isolation of blood leukocytes
  - scRNA-seq from blood leukocytes
  - Placenta dissection
  - snRNA-seq from decidua
  - Placenta histology
  - Flow cytometry on splenocytes
  - Autoantibody ELISAs
  - Serotonin ELISA
  - Genotyping
- QUANTIFICATION AND STATISTICAL ANALYSIS

SUPPLEMENTAL INFORMATION

Supplemental information can be found online at https://doi.org/10.1016/j.isci.2022.105595.

ACKOWLEDGMENTS

This work was supported by the the National Institutes of Health (1MH107535 and MH117004) to M.T. Portions of figures were created with BioRender.com. We'd also like to thank the following core facilities for their assistance in data collection and analysis: Laboratory of Comparative Pathology at Weill Cornell/ Memorial Sloan Kettering Cancer Center with support from funding by a P30 Core Grant, the Weill Cornell Research Animal Resource Center, the Weill Cornell Epigenomics Core, the Weill Cornell Applied Bioinformatics Core, and the Weill Cornell Microscopy and Imaging Core Facility.

AUTHOR CONTRIBUTIONS

Overall design of the study and conceptualization: R.C., H.S., A.B.P., and M.T., Experiments and analyses: R.J.C., A.N., S.P., D.F.C., J.G.T., P.B., J.B., H.S., A.B.P., and M.T., Writing – Original Draft: R.C., and M.T., Writing – Review and Editing: All authors.

DECLARATION OF INTEREST

The authors declare no competing interests.

INCLUSION AND DIVERSITY

We support inclusive, diverse, and equitable conduct of research.

Received: July 15, 2022
Revised: October 11, 2022
Accepted: November 10, 2022
Published: December 22, 2022

REFERENCES

1. Barnes, N.M., and Sharp, T. (1999). A review of central 5-HT receptors and their function. Neuropharmacology *38*, 1083–1152.

2. Garcia-Garcia, A.L., Newman-Tancredi, A., and Leonardo, E.D. (2014). 5-HT(1A) [corrected] receptors in mood and anxiety: recent insights into autoreceptor versus heteroreceptor function. Psychopharmacology (Berl) *231*, 623–636. https://doi.org/10.1007/s00213-013-3389-x.

3. Lanzenberger, R.R., Mitterhauser, M., Spindelegger, C., Wadsak, W., Klein, N., Mien, L.K., Holik, A., Attarbaschi, T., Mossaheb, N., Sacher, J., et al. (2007). Reduced serotonin-1A receptor binding in social anxiety disorder. Biol. Psychiatry *61*, 1081–1089.

4. Neumeister, A., Bain, E., Nugent, A.C., Carson, R.E., Bonne, O., Luckenbaugh, D.A., Eckelman, W., Herscovitch, P., Charney, D.S., and Drevets, W.C. (2004). Reduced serotonin type 1A receptor binding in panic disorder. J. Neurosci. *24*, 589–591.

5. Drevets, W.C., Thase, M.E., Moses-Kolko, E.L., Price, J., Frank, E., Kupfer, D.J., and Mathis, C. (2007). Serotonin-1A receptor imaging in recurrent depression: replication and literature review. Nucl. Med. Biol. *34*, 865–877.

6. Lemonde, S., Turecki, G., Bakish, D., Du, L., Hrdina, P.D., Bown, C.D., Sequeira, A., Kushwaha, N., Morris, S.J., Basak, A., et al. (2003). Impaired repression at a 5-hydroxytryptamine 1A receptor gene polymorphism associated with major depression and suicide. J. Neurosci. *23*, 8788–8799.

7. Donaldson, Z.R., le Francois, B., Santos, T.L., Almli, L.M., Boldrini, M., Champagne, F.A., Arango, V., Mann, J.J., Stockmeier, C.A., Galfalvy, H., et al. (2016). The functional serotonin 1a receptor promoter polymorphism, rs6295, is associated with psychiatric illness and differences in transcription. Transl. Psychiatry *6*, e746. https://doi.org/10.1038/tp.2015.226.

8. Wu, S., and Comings, D.E. (1999). A common C-1018G polymorphism in the human 5-HT1A receptor gene. Psychiatr. Genet. *9*, 105–106. https://doi.org/10.1097/00041444-199906000-00010.

9. Sullivan, G.M., Oquendo, M.A., Simpson, N., Van Heertum, R.L., Mann, J.J., and Parsey, R.V. (2005). Brain serotonin1A receptor binding in major depression is related to psychic and somatic anxiety. Biol. Psychiatry *58*, 947–954.

10. Huang, Y.Y., Battistuzzi, C., Oquendo, M.A., Harkavy-Friedman, J., Greenhill, L., Zalsman, G., Brodsky, B., Arango, V., Brent, D.A., and Mann, J.J. (2004). Human 5-HT1A receptor C(-1019)G polymorphism and psychopathology. Int. J. Neuropsychopharmacol. *7*, 441–451. https://doi.org/10.1017/S1461145704004663.

11. Sullivan, G.M., Ogden, R.T., Oquendo, M.A., Kumar, J.S.D., Simpson, N., Huang, Y.Y., Mann, J.J., and Parsey, R.V. (2009). Positron emission tomography quantification of serotonin-1A receptor binding in medication-free bipolar depression. Biol. Psychiatry *66*, 223–230.

12. Kaufman, J., Sullivan, G.M., Yang, J., Ogden, R.T., Miller, J.M., Oquendo, M.A., Mann, J.J., Parsey, R.V., and DeLorenzo, C. (2015). Quantification of the serotonin 1A receptor using PET: identification of a potential biomarker of major depression in males. Neuropsychopharmacology *40*, 1692–1699. https://doi.org/10.1038/npp.2015.15.

13. Parsey, R.V., Oquendo, M.A., Ogden, R.T., Olvet, D.M., Simpson, N., Huang, Y.Y., Van Heertum, R.L., Arango, V., and Mann, J.J. (2006). Altered serotonin 1A binding in major depression: a [carbonyl-C-11]WAY100635 positron emission tomography study. Biol. Psychiatry *59*, 106–113.

14. Czesak, M., Lemonde, S., Peterson, E.A., Rogaeva, A., and Albert, P.R. (2006). Cell-specific repressor or enhancer activities of Deaf-1 at a serotonin 1A receptor gene polymorphism. J. Neurosci. *26*, 1864–1871. https://doi.org/10.1523/JNEUROSCI.2643-05.2006.

15. Czesak, M., Le François, B., Millar, A.M., Deria, M., Daigle, M., Visvader, J.E., Anisman, H., and Albert, P.R. (2012). Increased serotonin-1A (5-HT1A) autoreceptor expression and reduced raphe serotonin levels in deformed epidermal autoregulatory factor-1 (Deaf-1) gene knock-out mice. J. Biol. Chem. *287*, 6615–6627. https://doi.org/10.1074/jbc.M111.293027.

16. Parks, C.L., Robinson, P.S., Sibille, E., Shenk, T., and Toth, M. (1998). Increased anxiety of mice lacking the serotonin(1A) receptor. Proc. Natl. Acad. Sci. USA *95*, 10734–10739. https://doi.org/10.1073/pnas.95.18.10734.

17. Ramboz, S., Oosting, R., Amara, D.A., Kung, H.F., Blier, P., Mendelsohn, M., Mann, J.J., Brunner, D., and Hen, R. (1998). Serotonin receptor 1A knockout: an animal model of anxiety-related disorder. Proc. Natl. Acad. Sci. USA *95*, 14476–14481.

18. Heisler, L.K., Chu, H.M., Brennan, T.J., Danao, J.A., Bajwa, P., Parsons, L.H., and Tecott, L.H. (1998). Elevated anxiety and antidepressant-like responses in serotonin 5-HT1A receptor mutant mice. Proc. Natl. Acad. Sci. USA *95*, 15049–15054.

19. Mitchell, E., Klein, S.L., Argyropoulos, K.V., Sharma, A., Chan, R.B., Toth, J.G., Barboza, L., Bavley, C., Bortolozzi, A., Chen, Q., et al. (2016). Behavioural traits propagate across generations via segregated iterative-somatic and gametic epigenetic mechanisms. Nat. Commun. *7*, 11492. https://doi.org/10.1038/ncomms11492.

20. Marrie, R.A., and Bernstein, C.N. (2021). Psychiatric comorbidity in immune-mediated inflammatory diseases. World Psychiatr. *20*, 298–299. https://doi.org/10.1002/wps.20873.

21. Marrie, R.A., Walld, R., Bolton, J.M., Sareen, J., Walker, J.R., Patten, S.B., Singer, A., Lix, L.M., Hitchon, C.A., El-Gabalawy, R., et al. (2017). Increased incidence of psychiatric disorders in immune-mediated inflammatory disease. J. Psychosom. Res. *101*, 17–23. https://doi.org/10.1016/j.jpsychores.2017.07.015.

22. Patterson, P.H. (2009). Immune involvement in schizophrenia and autism: etiology, pathology and animal models. Behav. Brain Res. *204*, 313–321.

23. Machado, C.J., Whitaker, A.M., Smith, S.E.P., Patterson, P.H., and Bauman, M.D. (2015). Maternal immune activation in nonhuman primates alters social attention in juvenile offspring. Biol. Psychiatry *77*, 823–832. https://doi.org/10.1016/j.biopsych.2014.07.035.

24. Kong, A., Thorleifsson, G., Frigge, M.L., Vilhjalmsson, B.J., Young, A.I., Thorgeirsson, T.E., Benonisdottir, S., Oddsson, A., Halldorsson, B.V., Masson, G., et al. (2018). The nature of nurture: effects of parental genotypes. Science *359*, 424–428. https://doi.org/10.1126/science.aan6877.

25. Gleason, G., Liu, B., Bruening, S., Zupan, B., Auerbach, A., Mark, W., Oh, J.E., Gal-Toth, J., Lee, F., and Toth, M. (2010). The serotonin(1A) receptor gene as a genetic and prenatal maternal environmental factor in anxiety. Proc. Natl. Acad. Sci. USA *107*, 7592–7597. https://doi.org/10.1073/pnas.0914805107.

26. van Velzen, A., and Toth, M. (2010). Role of maternal 5-HT1A receptor in programming offspring emotional and physical development. Genes Brain Behav. *9*, 877–885. https://doi.org/10.1111/j.1601-183X.2010.00625.x.

27. El-Brolosy, M.A., and Stainier, D.Y.R. (2017). Genetic compensation: a phenomenon in search of mechanisms. PLoS Genet. *13*, e1006780. https://doi.org/10.1371/journal.pgen.1006780.

28. Seidel, M.G. (2014). Autoimmune and other cytopenias in primary immunodeficiencies: pathomechanisms, novel differential diagnoses, and treatment. Blood *124*, 2337–2344. https://doi.org/10.1182/blood-2014-06-583260.

29. Keeling, D.M., and Isenberg, D.A. (1993). Haematological manifestations of systemic lupus erythematosus. Blood Rev. *7*, 199–207.

30. Ricker, E., Manni, M., Flores-Castro, D., Jenkins, D., Gupta, S., Rivera-Correa, J., Meng, W., Rosenfeld, A.M., Pannellini, T., Bachu, M., et al. (2021). Altered function and differentiation of age-associated B cells contribute to the female bias in lupus mice. Nat. Commun. *12*, 4813. https://doi.org/10.1038/s41467-021-25102-8.

31. Bronte, V., and Pittet, M.J. (2013). The spleen in local and systemic regulation of immunity. Immunity *39*, 806–818. https://doi.org/10.1016/j.immuni.2013.10.010.

32. Ueno, H., Banchereau, J., and Vinuesa, C.G. (2015). Pathophysiology of T follicular helper cells in humans and mice. Nat. Immunol. *16*, 142–152. https://doi.org/10.1038/ni.3054.

33. Phalke, S., Rivera-Correa, J., Jenkins, D., Flores Castro, D., Giannopoulou, E., and Pernis, A.B. (2022). Molecular mechanisms controlling age-associated B cells in autoimmunity. Immunol. Rev. *307*, 79–100. https://doi.org/10.1111/imr.13068.

34. Mildner, A., Schönheit, J., Giladi, A., David, E., Lara-Astiaso, D., Lorenzo-Vivas, E., Paul, F., Chappell-Maor, L., Priller, J., Leutz, A., et al. (2017). Genomic characterization of murine monocytes reveals C/EBPβ transcription factor dependence of Ly6C. Immunity *46*, 849–862.e7. https://doi.org/10.1016/j.immuni.2017.04.018.

35. Xie, X., Shi, Q., Wu, P., Zhang, X., Kambara, H., Su, J., Yu, H., Park, S.Y., Guo, R., Ren, Q., et al. (2020). Single-cell transcriptome profiling reveals neutrophil heterogeneity in homeostasis and infection. Nat. Immunol. *21*, 1119–1133. https://doi.org/10.1038/s41590-020-0736-z.

36. Rönnblom, L., and Eloranta, M.L. (2013). The interferon signature in autoimmune diseases. Curr. Opin. Rheumatol. *25*, 248–253. https://doi.org/10.1097/BOR.0b013e32835c7e32.

37. Rahim, M.M.A., Tu, M.M., Mahmoud, A.B., Wight, A., Abou-Samra, E., Lima, P.D.A., and Makrigiannis, A.P. (2014). Ly49 receptors: innate and adaptive immune paradigms. Front. Immunol. *5*, 145. https://doi.org/10.3389/fimmu.2014.00145.

38. Grieshaber-Bouyer, R., Radtke, F.A., Cunin, P., Stifano, G., Levescot, A., Vijaykumar, B., Nelson-Maney, N., Blaustein, R.B., Monach, P.A., and Nigrovic, P.A.; ImmGen Consortium (2021). The neutrotime transcriptional signature defines a single continuum of neutrophils across biological compartments. Nat. Commun. *12*, 2856. https://doi.org/10.1038/s41467-021-22973-9.

39. Maltepe, E., and Fisher, S.J. (2015). Placenta: the forgotten organ. Annu. Rev. Cell Dev. Biol. *31*, 523–552. https://doi.org/10.1146/annurev-cellbio-100814-125620.

40. Marsh, B., and Blelloch, R. (2020). Single nuclei RNA-seq of mouse placental labyrinth development. Elife *9*, e60266. https://doi.org/10.7554/eLife.60266.

41. Vento-Tormo, R., Efremova, M., Botting, R.A., Turco, M.Y., Vento-Tormo, M., Meyer, K.B., Park, J.E., Stephenson, E., Polański, K., Goncalves, A., et al. (2018). Single-cell reconstruction of the early maternal-fetal interface in humans. Nature *563*, 347–353. https://doi.org/10.1038/s41586-018-0698-6.

42. Simmons, D.G., Rawn, S., Davies, A., Hughes, M., and Cross, J.C. (2008). Spatial and temporal expression of the 23 murine Prolactin/Placental Lactogen-related genes is not associated with their position in the locus. BMC Genomics *9*, 352. https://doi.org/10.1186/1471-2164-9-352.

43. Sojka, D.K., Yang, L., and Yokoyama, W.M. (2019). Uterine natural killer cells. Front. Immunol. *10*, 960. https://doi.org/10.3389/fimmu.2019.00960.

44. Ain, R., Canham, L.N., and Soares, M.J. (2003). Gestation stage-dependent intrauterine trophoblast cell invasion in the rat and mouse: novel endocrine phenotype and regulation. Dev. Biol. *260*, 176–190. https://doi.org/10.1016/s0012-1606(03)00210-0.

45. Rai, A., and Cross, J.C. (2014). Development of the hemochorial maternal vascular spaces in the placenta through endothelial and vasculogenic mimicry. Dev. Biol. *387*, 131–141. https://doi.org/10.1016/j.ydbio.2014.01.015.

46. Simmons, D.G., Fortier, A.L., and Cross, J.C. (2007). Diverse subtypes and developmental origins of trophoblast giant cells in the mouse placenta. Dev. Biol. *304*, 567–578. https://doi.org/10.1016/j.ydbio.2007.01.009.

47. Woods, L., Perez-Garcia, V., and Hemberger, M. (2018). Regulation of placental development and its impact on fetal growth-new insights from mouse models. Front. Endocrinol. *9*, 570. https://doi.org/10.3389/fendo.2018.00570.

48. Li, Y., Xiao, B., Qiu, W., Yang, L., Hu, B., Tian, X., and Yang, H. (2010). Altered expression of CD4(+)CD25(+) regulatory T cells and its 5-HT(1a) receptor in patients with major depression disorder. J. Affect. Disord. *124*, 68–75. https://doi.org/10.1016/j.jad.2009.10.018.

49. Aune, T.M., McGrath, K.M., Sarr, T., Bombara, M.P., and Kelley, K.A. (1993). Expression of 5HT1a receptors on activated human T cells. Regulation of cyclic AMP levels and T cell proliferation by 5-hydroxytryptamine. J. Immunol. *151*, 1175–1183.

50. Xu, J., Zhang, G., Cheng, Y., Chen, B., Dong, Y., Li, L., Xu, L., Xu, X., Lu, Z., and Wen, J. (2011). Hypomethylation of the HTR1A promoter region and high expression of HTR1A in the peripheral blood lymphocytes of patients with systemic lupus erythematosus. Lupus *20*, 678–689. https://doi.org/10.1177/0961203310394892.

51. Abdouh, M., Storring, J.M., Riad, M., Paquette, Y., Albert, P.R., Drobetsky, E., and Kouassi, E. (2001). Transcriptional mechanisms for induction of 5-HT1A receptor mRNA and protein in activated B and T lymphocytes. J. Biol. Chem. *276*, 4382–4388. https://doi.org/10.1074/jbc.M004559200.

52. de Graaf, C.A., Choi, J., Baldwin, T.M., Bolden, J.E., Fairfax, K.A., Robinson, A.J., Biben, C., Morgan, C., Ramsay, K., Ng, A.P., et al. (2016). Haemopedia: an expression atlas of murine hematopoietic cells. Stem Cell Rep. *7*, 571–582. https://doi.org/10.1016/j.stemcr.2016.07.007.

53. Dahlin, J.S., Hamey, F.K., Pijuan-Sala, B., Shepherd, M., Lau, W.W.Y., Nestorowa, S., Weinreb, C., Wolock, S., Hannah, R., Diamanti, E., et al. (2018). A single-cell hematopoietic landscape resolves 8 lineage trajectories and defects in Kit mutant mice. Blood *131*, e1–e11. https://doi.org/10.1182/blood-2017-12-821413.

54. Tusi, B.K., Wolock, S.L., Weinreb, C., Hwang, Y., Hidalgo, D., Zilionis, R., Waisman, A., Huh, J.R., Klein, A.M., and Socolovsky, M. (2018). Population snapshots predict early haematopoietic and erythroid hierarchies. Nature *555*, 54–60. https://doi.org/10.1038/nature25741.

55. Hadden, J.W., Hadden, E.M., and Middleton, E. (1970). Lymphocyte blast transformation. I. Demonstration of adrenergic receptors in human peripheral lymphocytes. Cell. Immunol. *1*, 583–595. https://doi.org/10.1016/0008-8749(70)90024-9.

56. Pert, C.B., Ruff, M.R., Weber, R.J., and Herkenham, M. (1985). Neuropeptides and their receptors: a psychosomatic network. J. Immunol. *135*, 820s–826s.

57. Stamper, C.E., Hassell, J.E., Kapitz, A.J., Renner, K.J., Orchinik, M., and Lowry, C.A. (2017). Activation of 5-HT. Stress *20*, 223–230. https://doi.org/10.1080/10253890.2017.1301426.

58. Dhabhar, F.S. (2002). Stress-induced augmentation of immune function–the role of stress hormones, leukocyte trafficking, and cytokines. Brain Behav. Immun. *16*, 785–798. https://doi.org/10.1016/s0889-1591(02)00036-3.

59. Eddy, J.L., Krukowski, K., Janusek, L., and Mathews, H.L. (2014). Glucocorticoids regulate natural killer cell function epigenetically. Cell. Immunol. *290*, 120–130. https://doi.org/10.1016/j.cellimm.2014.05.013.

60. Ngampramuan, S., Baumert, M., Beig, M.I., Kotchabhakdi, N., and Nalivaiko, E. (2008). Activation of 5-HT(1A) receptors attenuates tachycardia induced by restraint stress in rats. Am. J. Physiol. Regul. Integr. Comp. Physiol. *294*, R132–R141. https://doi.org/10.1152/ajpregu.00464.2007.

61. Vantrease, J.E., Dudek, N., DonCarlos, L.L., and Scrogin, K.E. (2015). 5-HT1A receptors of the nucleus tractus solitarii facilitate sympathetic recovery following hypotensive hemorrhage in rats. Am. J. Physiol. Heart Circ. Physiol. *309*, H335–H344. https://doi.org/10.1152/ajpheart.00117.2015.

62. Reinhold, K. (2002). Maternal effects and the evolution of behavioral and morphological characters: a literature review indicates the importance of extended maternal care. J. Hered. *93*, 400–405. https://doi.org/10.1093/jhered/93.6.400.

63. Mitchell, C., Notterman, D., Brooks-Gunn, J., Hobcraft, J., Garfinkel, I., Jaeger, K., Kotenko, I., and McLanahan, S. (2011). Role of mother's genes and environment in postpartum depression. Proc. Natl. Acad. Sci. USA *108*, 8189–8193.

64. Song, H., Fang, F., Tomasson, G., Arnberg, F.K., Mataix-Cols, D., Fernández de la Cruz, L., Almqvist, C., Fall, K., and Valdimarsdóttir, U.A. (2018). Association of stress-related disorders with subsequent autoimmune disease. JAMA *319*, 2388–2400. https://doi.org/10.1001/jama.2018.7028.

65. Siegmann, E.M., Müller, H.H.O., Luecke, C., Philipsen, A., Kornhuber, J., and Grömer, T.W. (2018). Association of depression and anxiety disorders with autoimmune thyroiditis: a systematic review and meta-analysis. JAMA Psychiatr. *75*, 577–584. https://doi.org/10.1001/jamapsychiatry.2018.0190.

66. Howerton, C.L., and Bale, T.L. (2012). Prenatal programing: at the intersection of maternal stress and immune activation. Horm. Behav. *62*, 237–242. https://doi.org/10.1016/j.yhbeh.2012.03.007.

67. Akimova, E., Lanzenberger, R., and Kasper, S. (2009). The serotonin-1A receptor in anxiety disorders. Biol. Psychiatry *66*, 627–635. https://doi.org/10.1016/j.biopsych.2009.03.012.

68. Lesch, K.P., Wiesmann, M., Hoh, A., Müller, T., Disselkamp-Tietze, J., Osterheider, M., and Schulte, H.M. (1992). 5-HT1A receptor-effector system responsivity in panic disorder. Psychopharmacology (Berl) *106*, 111–117.

69. Tauscher, J., Bagby, R.M., Javanmard, M., Christensen, B.K., Kasper, S., and Kapur, S. (2001). Inverse relationship between serotonin 5-HT(1A) receptor binding and anxiety: a [(11)C]WAY-100635 PET investigation in healthy volunteers. Am. J. Psychiatry *158*, 1326–1328.

70. Haddad, J.J., Saadé, N.E., and Safieh-Garabedian, B. (2002). Cytokines and neuro-immune-endocrine interactions: a role for the hypothalamic-pituitary-adrenal revolving axis. J. Neuroimmunol. *133*, 1–19.

71. Fung, T.C., Olson, C.A., and Hsiao, E.Y. (2017). Interactions between the microbiota, immune and nervous systems in health and disease. Nat. Neurosci. *20*, 145–155. https://doi.org/10.1038/nn.4476.

72. Elenkov, I.J., Wilder, R.L., Chrousos, G.P., and Vizi, E.S. (2000). The sympathetic nerve–an integrative interface between two supersystems: the brain and the immune system. Pharmacol. Rev. *52*, 595–638.

73. Connor, T.J., Song, C., Leonard, B.E., Merali, Z., and Anisman, H. (1998). An assessment of the effects of central interleukin-1beta, -2, -6, and tumor necrosis factor-alpha administration on some behavioural, neurochemical, endocrine and immune parameters in the rat. Neuroscience *84*, 923–933.

74. Tunster, S.J. (2017). Genetic sex determination of mice by simplex PCR. Biol. Sex Differ. *8*, 31. https://doi.org/10.1186/s13293-017-0154-6.

STAR★METHODS

KEY RESOURCES TABLE

REAGENT or RESOURCE	SOURCE	IDENTIFIER
Antibodies		
B220 (RA3-6B2)-PE	Biolegend	Cat# 103208
B220 (RA3-6B2)-PE/Cy7	Biolegend	Cat# 103222
B220 (RA3-6B2)-FITC	Biolegend	Cat# 103206
B220 (RA3-6B2)-FITC	Biolegend	Cat# 103227
CD93 (AA4.1)-APC	Biolegend	Cat# 136510
CD3 (145-2C11)-PE	Biolegend	Cat# 100308
CD4 (RM4-5)-APC	Biolegend	Cat# 100526
CD8 (53-6.7)-A700	Biolegend	Cat# 100730
CD11b (M1/70)-FITC	Biolegend	Cat# 101206
CD11c (N418)-APC/fire	Biolegend	Cat# 117352
CD19 (6D5)-PB	Biolegend	Cat# 115523
CD19 (6D5)-PE	Biolegend	Cat# 115508
CD21 (7E9)-FITC	Biolegend	Cat# 123408
CD23 (B3B4)-PCP	Biolegend	Cat# 101618
CD44 (IM7)-PCP	Biolegend	Cat# 103032
CXCR3 (CXCR3-173)-A700	Biolegend	Cat# 126542
T-bet (4B10)-PE/Cy7	Biolegend	Cat# 644824
CD138 (281-2)-APC	BD Biosciences	Cat# 142506
Biotin Rat Anti-mouse CXCR5 (2G8)	BD Biosciences	Cat# 551960
Biotin Hamster Anti-Mouse CD95 (Jo2)	BD Biosciences	Cat# 554256
GL7 (GL7)-PE	Biolegend	Cat# 144608
Foxp3 (MF-14)-PB	Biolegend	Cat# 126410
PD1 (EH12.2H7)-FITC	Biolegend	Cat# 329935
HRP-labeled goat anti-mouse IgG	SouthernBiotech	Cat# 1030-05
HRP-labeled goat anti-mouse IgG2c	SouthernBiotech	Cat# 1079-05
rabbit anti-TPBPA polyclonal	Abcam	Cat#104401
rat anti-CD31 monoclonal	BD Pharmingen Biosciences	Cat#553370
goat anti-rabbit AF555 polyclonal	Abcam	Cat#ab150078
goat anti-rat AF488 polyclonal	Jackson ImmunoResearch	Cat#112-545-167
goat anti-rat Cy5 polyclonal	Jackson ImmunoResearch	Cat#112-175-167
Chemicals, peptides, and recombinant proteins		
Ficoll-Paque PREMIUM 1.084	Cytiva	Cat#17-5446-02
RBC Lysis Buffer	eBioscience	Cat#2165448
Nuclei EZ lysis buffer	Sigma-Aldrich	Cat#NUC101
Protector RNase inhibitor	Roche	Cat#3335399001
salmon sperm DNA	Invitrogen	Cat#AM9680
Cardiolipin sodium salt from bovine heart, ≥98% (TLC), lyophilized powder	Sigma-Aldrich	Cat# C0563-10MG
1,2-Diacyl-*sn*-glycero-3-phospho-L-serine, ≥97% (TLC), from bovine brain, amorphous powder	Sigma-Aldrich	Cat# P7769-5MG
Tissue-Tek OCT compound	Sakura Finetek USA	Cat#4583

(*Continued on next page*)

Continued

REAGENT or RESOURCE	SOURCE	IDENTIFIER
Critical commercial assays		
Chromium Single Cell 3′ Reagent V3 Kit	10X Genomics	N/A
Mouse Corticosterone ELISA Kit	Enzo	Cat#ADI-901-097
eBioscience™ Foxp3/Transcription Factor Staining Buffer Set	Thermo Fisher Scientific	Cat# 00-5523-00
Mouse Serotonin ELISA Kit	Enzo Life Sciences	Cat# ADI-900-175
Pro-Long Diamond Antifade Mountant with DAPI	Invitrogen	Cat#P36962
CoverGrip Coverseal Sealant	Biotium	Cat#23005
DPX Mountant	Sigma	Cat#06522
Deposited data		
scRNA-seq data from gestation day 10.5 peripheral leukocytes (from WT and heterozygote 5HT1AR KO female mice) and snRNA-seq data from gestation day 10.5 decidual cell nuclei (from WT and heterozygote 5HT1AR KO mice)	GSE217086	
Experimental models: Organisms/strains		
5HT1AR KO Swiss Webster mice	Parks et al., 1998[16]	N/A
Oligonucleotides		
Primer for Rbm31, Forward: CACCTTAAGAACAAGCCAATACA	Tunster, 2017[74]	N/A
Primer for Rbm31, Reverse: GGCTTGTCCTGAAAACATTTGG	Tunster, 2017[74]	N/A
Software and algorithms		
Noldus Ethovision XT	Noldus Information Technology	N/A
Graphpad Prism 9	Graphpad	N/A
IDEXX Pro-Cyte Dx Hematology Analyzer	IDEXX	N/A
FlowJo 10.5.2	FlowJo	N/A
Other		
Microtainer K2EDTA blood collection tubes	BD Biosciences	Cat#365974
Fisherbrand Superfrost Plus slides	Fisher Scientific	Cat#12-550-15

RESOURCE AVAILABILITY

Lead contact

Further information and requests for resources and reagents should be directed to and will be fulfilled by the lead contact, Miklos Toth (mtoth@med.cornell.edu).

Materials availability

This study did not generate new unique reagents.

Data and code availability

Single-cell RNA-seq data are deposited to the NCBI GEO and will be publicly available at the time of publication. Accession numbers are listed in the key resources table.

Microscopy data reported in this paper will be shared by the lead contact upon request.

This paper does not report original code.

Any additional information required to reanalyze the data reported in this paper is available from the lead contact upon request.

EXPERIMENTAL MODEL AND SUBJECT DETAILS

In vivo animal studies

All animal experiments were carried out in strict accordance with the National Institutes of Health guidelines under protocols approved by the Weill Cornell Medical College Institutional Animal Care and Use Committee. All mice were group-housed two to five per cage, with a 12-h light/dark cycle and lights on at 6 a.m. Food and water were available *ad libitum*. 5HT1AR homozygote KO mice were originally generated on the 129Sv background and backcrossed to the Swiss Webster strain (Taconic Biosciences) as previously described.[16]

METHOD DETAILS

Timed pregnancies

All females used for time pregnancies were virgin females between 10 and 12 weeks of age. All males used for timed pregnancies were between 10 and 16 weeks of age and included virgin and non-virgin males. Timed pregnancies were generated by housing two naturally cycling females with a single male overnight. Successful copulation was assessed at 9 a.m. the following morning by the appearance of a vaginal plug (noon of plug detection is gestational day 0.5, GD0.5). Successfully plugged females were removed and singly housed for the remainder of the pregnancy.

Complete blood count

All mice used for complete blood count were virgin adults (10–16 weeks of age), of both sexes. After terminal anesthesia by pentobarbital, ~100 μL peripheral whole blood was collected via cardiac puncture and transferred into BD Microtainer K2EDTA blood collection tubes (BD 365974). Total red blood cells, platelets, reticulocytes, WBCs, neutrophils, lymphocytes, monocytes, eosinophils and basophils were quantified by automated (IDEXX Pro-Cyte Dx Hematology Analyzer) counts. All animals used for CBC were virgin animals between 10 and 16 weeks of age.

Isolation of blood leukocytes

N = 4 non-sister female mice at GD10.5 were processed per group (WT and Het). After terminal anesthesia by pentobarbital, maximum peripheral whole blood (~2 mL) was collected via cardiac puncture and stabilized in BD Microtainer K2EDTA blood collection tubes. Biological replicates from each group were then pooled together and an equal volume of 1X DPBS without magnesium or calcium (Gibco 14190144) was added to the whole blood. The diluted whole blood was layered onto Ficoll-Paque PREMIUM 1.084 (Cytiva 17-5446-02) (2 parts blood to 3 parts Ficoll in volume). The gradient was spun at 400 x g for 30 min with the brakes off at room temperature (RT). Plasma was removed and the layer containing peripheral blood mononuclear cell (PBMC) was collected and transferred to a new tube. The remaining Ficoll layer was removed, and the RBC/granulocyte pellet was suspended in 1X RBC Lysis Buffer (eBioscience 2165448) in a 1:10 ratio. The solution was gently inverted a few times, incubated at RT for 15 min, then spun at 300 × g for 5 min with brakes on low at RT. The supernatant with lysed RBC fragments was removed. The pellet was washed with a volume of DPBS equal to the amount of RBC Lysis Buffer used and spun at 350 × g with brakes on low for 5 min at RT. Wash was repeated, the supernatant was removed, and the resulting pellet of granulocytes was resuspended in 1 mL DPBS with 2% FBS and set on ice. Separately, the volume of collected PBMC was estimated and 4X that volume of DPBS was added to the PBMC fraction. The sample was gently triturated with a serological pipet, then spun at 400 × g for 10 min with brakes on low at RT. RBC lysis buffer was added to the pellet as above and the resulting pellet was washed twice with DPBS. Final PBMC pellet was resuspended in 1 mL DPBS with 2% FBS, combined with granulocyte suspension, and visually inspected with a hemocytometer under a microscope for cell counting.

scRNA-seq from blood leukocytes

Final single cell suspensions, as prepared above, were submitted to the Weill Cornell Epigenomic Core for library preparation and sequencing. Sample libraries were prepared using the Chromium Single Cell 3′

Reagent V3 Kit from 10X Genomics according to manufacturer instructions. Libraries were sequenced on an Illumina NovaSeq to a depth of approximately 25,000–30,000 mean reads per cell. FASTQ files were processed using the CellRanger v5.0.0 pipeline and aligned to the mm10 transcriptome. Gene-expression matrices of Het and WT samples were separately loaded into R and merged using Seurat. Cells with fewer than 200 genes and more than 4000 genes, greater than 10% mitochondrial gene reads and 25% hemoglobin gene reads were filtered out. Genes expressed in fewer than 5 cells were also excluded from the matrix. The merged matrix was normalized and log-transformed using NormalizeData. 2,000 variable genes were identified and scaled for principal component analysis (PCA) using FindVariableFeatures and ScaleData. Following PCA, clusters were identified and visualized on UMAP using the FindNeighbors, FindClusters, and RunUMAP functions with 20 principal components (PCs) and a resolution of 1. Cluster markers were identified with the FindAllMarkers function (min.pct = 0.25) using the Wilcoxin rank-sum test and pvalues were adjusted using Bonferroni correction. Following annotation of clusters, two T cell clusters were subclustered using the FindSubcluster function with resolutions of 0.2 and 0.3. Any clusters expressing multiple cell-type markers or expressing a high percentage of mitochondrial/hemoglobin genes, low number of UMIs and an overall low number of genes were excluded from downstream analysis. To further exclude doublets, non-platelet cells expressing *Itga2b*> 1, non-neutrophil cells expressing *S100a8* or *S100a9*> 4, non-T-cells expressing *Cd3e*> 1, non-NK cells expressing *Ncr1*> 1, non-cycling cells expressing *Mki67*> 1 and non-Cd8+ T-cells expressing *Cd8b1*> 1 were removed. All preprocessing steps starting with normalization were rerun as described above with 30 PCs and a resolution of 0.6 used for clustering. One B-cell cluster, one monocyte cluster and two T cell clusters were also subclustered. Cluster markers were re-identified using the previously used function and parameters. In addition, cluster specific differential expression was also found using the FindMarkers function (min.pct = 0.25) with the Wilcoxon rank-sum test and Bonferroni correction (adjusted pvalue < 0.05 and a fold change >1.5).

Placenta dissection

All mice used for placenta dissection were primiparous females (10–12 weeks of age). After terminal anesthesia by pentobarbital, a midline incision was made on the lower abdomen and the uterine horns were removed and transferred to a Petri dish of cold DPBS on ice. Each conceptus was carefully cut away from the uterine horn. Fine forceps and scissors were used to make small incisions in the uterine wall and the fetoplacental unit was removed from the uterine wall. A small incision was made in the chorioallantoic membrane encasing the fetus and the placenta was separated at the basal chorionic plate. In GD10.5 placenta, isolation of the decidua was achieved by flipping the placenta so that the flat fetal labyrinth was facing up and the tissue was resting on its convex maternal decidual side. Fine forceps grasped the outside ring of the maternal decidua visualized from the flat labyrinth layer, while another pair of fine forceps gently dug into and separated the labyrinth layer in a gentle scooping motion. In GD17.5 placenta, fine tipped forceps were slipped between the white decidual tissue layer and the placenta layer and the decidual tissue was gently peeled from the placenta surface. All excess uterine membranes were trimmed. Placentas were gently blotted with a Kimwipe and weighed. Tissue identity was confirmed by PCR targeting the *Dlx3* gene, as described below. The fetus (whole, if < GD13.5; only the fetal tail, if > GD13.5) was stored in a tube for DNA extraction for sex genotyping.

snRNA-seq from decidua

N = 3 decidua from non-sibling placenta at GD10.5 were processed per group (WT and Het decidua from WT and F1 placenta). Single nuclei suspension was prepared from frozen tissue with slight modifications to the method described by Marsh and Blelloch 2020.[40] In brief, 1 mL prechilled Nuclei EZ lysis buffer (Sigma-Aldrich NUC101) was added to each flash-frozen decidua sample, which was then minced finely with dissection scissors. A wide bore pipet was used to transfer pooled minced tissue into a glass Dounce homogenizer. Tissue was lysed with 20 strokes of the loose pestle followed by 20 strokes of the tight pestle. The homogenate was transferred to a new tube and an additional 3 mL of prechilled Nuclei EZ Lysis Buffer was added. The sample was incubated on ice for 5 min and was resuspended a few times throughout. The lysate was filtered through a 70 μM filter and spun at 500 x g for 5minat 4°C in a centrifuge with a swinging bucket rotor. The supernatant was removed, and the pellet was resuspended with 2 mL Nuclei EZ Lysis Buffer and incubated for an additional 5 min on ice. The sample was spun at 500 × g for 5minat 4°C and the supernatant was removed. 1 mL Nuclei Wash Buffer (DPBS without magnesium and calcium, 2% BSA, and 0.2U Protector RNase inhibitor [Roche 3335399001]) was layered onto the pellet and the sample was incubated on ice for 5 min without mixing or resuspending to promote buffer exchange. An additional 2 mL Nuclei Wash Buffer was used to resuspend, and the sample was spun at 500 x g for 5 min at 4°C. The

lysate was removed, and this wash step was repeated. Finally, the pellet was resuspended in 1.5 mL Nuclei Wash Buffer, filtered through a 70 μM filter, and visually inspected with a hemocytometer under a microscope for cell counting.

Final samples consisted of 1 × 10^6 nuclei in 100 μL and were submitted to the Weill Cornell Epigenomic Core for library preparation using the Chromium Single Cell 3′ Reagent V3 Kit and sequencing via Illumina Novaseq, as described above for scRNA-Seq. Libraries were sequenced to a depth of approximately 20,000 mean reads per nuclei. Raw sequencing data were processed using the CellRanger v6.0.0 pipeline and aligned to the mm10 transcriptome with introns included in the reference. Gene-expression matrices of both samples were loaded into R and preprocessed separately using Seurat. Nuclei with fewer than 500 genes and greater than 5% ribosomal gene reads, and genes expressed in fewer than 5 nuclei were filtered out. Preprocessing steps described above were then used to normalize and cluster nuclei. 20 PCs and a resolution of 1.8 was used to cluster the WT sample while 20 PCs and a resolution of 1.2 was used to cluster the Het sample. Following exclusion of low-quality clusters, preprocessing steps were rerun. The WT sample was reclustered using 20 PCs and a resolution of 1.2. The Het sample was reclustered using 20 PCs and a resolution of 1.4, and an additional low-quality cluster was removed. Following reclustering, doublets were detected using DoubletFinder (https://github.com/chris-mcginnis-ucsf/DoubletFinder/blob/master/README.md) (8% expected doublet rate, 20 PCs and pK = 0.005 for WT and pK = 0.14 for Het).

Singlets with fewer than 4000 genes were then merged into one gene-expression matrix and normalized using SCTranform() with mitochondrial genes regressed out. Following PCA, clustering (40 PCs and resolution = 0.5) and subclustering of a DSC cluster (resolution = 0.1), cluster markers and cluster specific differentially expressed genes were identified using the parameters described above. Differences in the proportions of nuclei per cluster between WT and Het samples was analyzed by permutation testing (10,000 permutations) using the scProportionTest package (https://github.com/rpolicastro/scProportionTest).

Placenta histology

Whole intact placentas dissected as above were post-fixed in 4% PFA at 4°C overnight, then transferred to a 30% sucrose solution until water displacement was visually confirmed (typically overnight), gently rinsed in DPBS, then embedded in plastic molds with Tissue-Tek OCT compound (Sakura Finetek USA 4583) with the flat labyrinth side at the base of the mold and the convex decidua surface facing the top. The embedded tissue molds were stored at −80°C until all samples were ready to be processed. When the tissue was ready to be cut, the frozen tissue in the mold was brought to −20°C inside the cryostat chamber and cut into 10 μm sections at −20°C. Tissue sections were mounted directly onto Fisherbrand Superfrost Plus slides (Fisher Scientific 12-550-15) and air dried at room temperature in front of a small desktop fan for at least 30 min prior to being stored at −80°C. To prepare the slides for histological staining, slides were removed from −80°C and dried for 20minat RT in front of a small desktop fan. Sections were outlined with a PAP pen (Enzo ADI-950-233-001).

For immunohistochemistry, slides were prepared as follows. Slides were rinsed 3X with TB for 10 min and then 3X with TBS for 10 min. Slides were blocked with 5% goat serum, 0.2% Triton X-100 in TBS for 1hat RT. Slides were rinsed 2X with TBS for 5 min. Slides were incubated in primary antibodies overnight at 4°C in 5% goat serum and 0.1% Triton X-100 in TBS. Primary antibodies were as follows: rabbit anti-TPBPA 1:100 (Abcam 104401) and rat anti-CD31 1:100 (BD Pharmingen Biosciences 553370). On day 2, samples were rinsed 6X with TBS for 10 min. Slides were incubated with secondary antibodies in the dark for 1hat RT in 5% goat serum, 0.1% Triton X-100 in TBS. Secondary antibodies were as follows: goat anti-rabbit AF555 1:1000 (Abcam, ab150078) and goat anti-rat AF488 and Cy5 1:1000 (Jackson ImmunoResearch, 112-545-167 and 112-175-167). Slides were rinsed in the dark for 5X with TBS for 10 min, then once with TB for 10 min. Slides were cover slipped in the dark using Pro-Long Diamond Antifade Mountant with DAPI (Invitrogen P36962). Cover glass was sealed with CoverGrip Coverseal Sealant (Biotium 23005) and slides were stored in the dark at 4°C short term and at −20°C long term.

For H&E staining, slides were prepared as follows. Fan-dried slides were rehydrated by transferring the slides through three changes of 100% ethanol (EtOH) chambers for 2 min per change. Slides were transferred to 95% EtOH for 2 min, then 70% EtOH for 2 min. Slides were rinsed in running tap water at RT for at least 2 min. Slides were stained in hematoxylin solution for 30 s by a brief dip. Slides were placed

under running tap water at RT for at least 5 min. Slides were then stained in working eosin Y solution for 20 s by a brief dip. Samples were then repeatedly dipped in a tap water chamber 20X. Samples were dehydrated by dipping the slides in 95% EtOH 20X, then 85% EtOH for 2 min, then transferred through two changes of 100% EtOH for 2 min per change. Samples were cleared in three changes of xylene for 2 min per change. Slides were cover slipped using DPX Mountant for histology (Sigma 06522). Stained sections were imaged on a Nikon Eclipse TE200 Inverted or a Nikon Eclipse 80i Fluorescence Microscope. N = 4 placentas were stained for each group and one representative image per group was chosen.

Flow cytometry on splenocytes

After isoflurane anesthesia and cervical dislocation euthanasia, spleens were collected from 31-week-old female WT, Het, and F1 mice and transferred to FACS buffer (500 mM EDTA, 2% FBS, in 1X DPBS without magnesium or calcium). Spleen were gently mashed with the plunger of a 3 mL syringe on top of a 45 μm filter into a 50 μL Falcon tube with 15 mL FACS buffer. The suspension was spun down at 1500 rpm for 4minat 4°C. The supernatant was removed, and the remaining pellet was resuspended in 2 mL RBC lysis buffer. After a 5-min incubation at 4°C, the suspension was brought up to 10 mL with FACS buffer and run through a 45 μm filter into a 50 mL Falcon tube. The filter was rinsed with an additional 10 mL FACS buffer. The suspension was spun down at 1500 rpm for 4minat 4°C. The supernatant was discarded, and the cells were resuspended in 10 mL of FACS buffer for counting by a hemocytometer. Splenocytes were diluted to 1.5×10^6/well and stained in 96-well plates (Falcon, BD Biosciences) with the following monoclonal antibodies for multi-parameter flow cytometry: B220 (RA3-6B2, 400x), CD93 (AA4.1, 800X), CD3 (145-2C11, 800X), CD4 (RM4-5; 400x), CD8 (53-6.7, 400X), CD11b (M1/70; 400x), CD11c (N418; 400x), CD19 (HIB19; 400x), CD21 (7E9; 200x), CD23 (B3B4; 200x), CD44 (IM7; 200x), CXCR3 (CXCR3-173; 200x), and T-bet (4B10; 800x), all obtained from BioLegend. Streptavidin-conjugated antibodies were also obtained from BioLegend. Antibodies to CD138 (281-2; 1200x), CXCR5 (2G8; 200x), Fas (Jo2; 200x) and GL7 (600x) were obtained from BD. Antibodies to Foxp3 (FJK-16s; 100x) and PD1 (J43; 200x) were obtained from eBioscience. For intracellular staining, cells were fixed after surface staining at 4°C with the Transcription Factor Staining Kit (eBioscience) per the manufacturer's instructions. Samples were analyzed using BD FACSCanto flow cytometer (Becton Dickinson). At least 1×10^5 events were acquired per gated region, and the data were analyzed using FlowJo 10.5.2 software (TreeStar).

Autoantibody ELISAs

All mice used for autoantibody ELISAs were adults females (12–16 weeks of age). After terminal anesthesia by pentobarbital, ~ 1 mL peripheral whole blood was collected via cardiac puncture. Sera were stored at −80°C until all samples were ready for processing. For the anti-dsDNA ELISA, plates were coated with 100 μg/mL salmon sperm DNA (Invitrogen; AM9680) at 37°C overnight and blocked in 2% BSA in PBS at RT for 2 h. For the anti-cardiolipin and anti-phosphatidylserine ELISAs, Immulon 2HB plates (Thermo Fisher) were coated overnight with 75 μg/mL of cardiolipin or with 30 μg/mL phosphatidylserine dissolved in 100% ethanol. Sera were diluted 1:200 and incubated on coated plates at 25°C for 2 h. Plates were then incubated with HRP-labeled goat anti-mouse IgG or IgG2c Fc antibody (eBioscience) for 1 h. Optical density (O.D.) at 450 nm wavelength was measured on a microplate reader.

Serotonin ELISA

All mice used for serotonin ELISAs were adults (10–16 weeks of age), of both sexes. After terminal anesthesia by pentobarbital, 1 mL peripheral whole blood was collected via cardiac puncture and stabilized in BD Microtainer K2EDTA blood collection tubes on ice. Blood samples were spun at 100 x g for 15minat RT and the resulting platelet rich plasma supernatant layer was collected and stored at −80°C until all samples were ready for testing.

Genotyping

Allelic genotyping for the serotonin 1A receptor gene (*Htr1a*) was performed as previously described.[16,25] To determine the sex and genotype of the fetal placenta, dissected embryos were enzymatically digested using DirectPCR Lysis Reagent (Viagen 102T) and Proteinase K (Thermo Fisher Scientific, 4333793) and DNA was extracted. Primers used for sex genotyping PCR-target the *Rbm31* gene[74] (Forward primer: CACCTT AAGAACAAGCCAATACA; reverse primer: GGCTTGTCCTGAAAACATTTGG). In a 1.5% agarose gel run for 30 min at 110 V, female samples resolve a single band at 269 bp while male samples resolve two bands at 269 bp and 353 bp.

QUANTIFICATION AND STATISTICAL ANALYSIS

Data from animal studies were compiled in Microsoft Excel and analyzed using Prism 9.0 software or R. Scatterplots utilize small dots to represent individual animals and large dots to indicate litter/maternal average. Bar graphs are shown as litter/maternal mean ±SE of mean (SEM). If there is only one size dot, they represent individual mice, and the associated bar graph is mean ±SEMof individuals. Outlier data were excluded based on 2 standard deviations (SD) from the mean. One or two-way ANOVAs on litter/maternal averages, unless otherwise specified, were followed by Tukey or Dunnett corrections for multiple comparisons. *$p < 0.05$, **$p < 0.01$, ***$p < 0.001$, ****$p < 0.0001$. Sample sizes were estimated using post-hoc power analyses from similar previously conducted studies.